Zeitschrift: Schweizerische mineralogische und petrographische Mitteilungen = Bulletin suisse de minéralogie et pétrographie

Band: 67 (1987)

Heft: 3

Artikel: The HP-LT manganiferous quartzites of Praborna, Piemonte ophiolite nappe, Italian Western Alps

Autor: Martin, Silvana / Kienast, Jean Robert

DOI: https://doi.org/10.5169/seals-51609

Nutzungsbedingungen

Die ETH-Bibliothek ist die Anbieterin der digitalisierten Zeitschriften. Sie besitzt keine Urheberrechte an den Zeitschriften und ist nicht verantwortlich für deren Inhalte. Die Rechte liegen in der Regel bei den Herausgebern beziehungsweise den externen Rechteinhabern. Siehe Rechtliche Hinweise.

Conditions d'utilisation

L'ETH Library est le fournisseur des revues numérisées. Elle ne détient aucun droit d'auteur sur les revues et n'est pas responsable de leur contenu. En règle générale, les droits sont détenus par les éditeurs ou les détenteurs de droits externes. Voir Informations légales.

Terms of use

The ETH Library is the provider of the digitised journals. It does not own any copyrights to the journals and is not responsible for their content. The rights usually lie with the publishers or the external rights holders. See Legal notice.

Download PDF: 10.11.2024

ETH-Bibliothek Zürich, E-Periodica, https://www.e-periodica.ch

SCHWEIZ. MINERAL. PETROGR. MITT. 67, 339-360, 1987

The HP-LT manganiferous quartzites of Praborna, Piemonte ophiolite nappe, Italian Western Alps

by *Silvana Martin*[1] and *Jean Robert Kienast*[2]

Abstract

The Praborna manganiferous deposit is located in the middle St. Marcel valley (Aosta region). It occurs in the quartzitic basal part of the metasedimentary cover overlying an ophiolitic sequence of oceanic affinity from the metamorphic Piemonte nappe.

The mineralized sequence consists of several alternating siliceous lithologies, generated by the mixing of biogenic radiolarian ooze and hydrothermal silica, with minor metabasalts, metapelitic and quartzofeldspathic schists, and is characterized by different mineral assemblages, fO_2, texture and colour.

The lower parts of the manganiferous series are mainly composed of pyroxene-bearing quartzites and aegirine-jadeite / chloromelanite-bearing pyroxenites including the major Mn-orebody constituted by predominant braunite ± hausmannite and pyrolusite (secondary).

The upper parts are composed of micaschists, sometimes carbonatic or more quartzitic including bands of Mn silicates (spessartine, piemontite, Mn-phengite) and lenses of Mn-oxides intercalated with bands rich in Fe-silicate (epidote, clinopyroxene) and hematite. A chromiferous quartzite including Cr-aegirine-augite, uvarovite and hematite is associated with the manganiferous sequence.

Several vein generations crosscut the Mn orebody, the associated quartzites, pyroxenites and the overlying metabasites. Veins related to the braunite ± hausmannite bodies are filled with purple-blue pyroxene (violan), piemontite, albite, ± Mn-sphene (greenovite) or with rhodochrosite, with rhodonite, with K-Mn-richterite and quartz.

The Praborna deposit shows superposed metamorphic phases related to the alpine subduction and exhumation processes. Traces of the prograde assemblages of pre-eclogitic blueschist-facies metamorphism (early Cretaceous) are scarcely preserved.

Polyphase HP assemblages of the Cretaceous event record T ranging from 450 °C to 500 °C and P from 8 to above 10 kbar.

Assemblages from albite-epidote amphibolite to greenschist facies of the meso-Alpine (Eocene-lower Oligocene) metamorphic overprinting are widespread in the basic rocks surrounding the deposit and in the metapelitic rocks associated with the Mn-orebodies.

Keywords: Manganiferous sequence, Mn-ores, HP-metamorphism, ophiolite nappe, Praborna, Italian Alps.

[1] Istituto di Geologia dell'Università, Via Giotto 1, 35100 Padova, Italy.

[2] Jean Robert Kienast, Pétrologie métamorphique, Université Pierre et Marie Curie, 4, Place Jussieu, 75230 Paris, Cédex 05.

Abbreviations

Acm	acmite	Ktn	kutnahorite
Aeg	aegirine	Mi	microcline
Aeg-aug	aegirine-augite	Ms	muscovite
Aeg-jd	aegirine-jadeite	Na-amph	Na-amphibole
Alm	almandine	Omph	omphacite
Alu	alurgite	Phe	phengite
And	andradite	Phl	phlogopite
Aug	augite	Pm	piemontite
Brn	braunite	Prs	pyrolusite
Ca-amph	Ca-amphibole	Ps	pistacite
Cc	calcite	Pyr	pyrophanite
Chlm	chloromelanite	Pxm	pyroxmangite
Cpx	clinopyroxene	Rt	richterite
Ep	epidote	Rdc	rhodochrosite
Gt	garnet	Rhd	rhodonite
Hem	hematite	Sp	spessartine
Jd	jadeite	Tr	tremolite
Krp	kryptomelane	Uv	uvarovite
K-Rt	potassium-richterite	Win	winchite

1. Introduction

The Praborna deposit, forming the most interesting manganiferous concentration associated with the supraophiolitic metasedimentary cover in the Piemonte nappe, is located in the St. Marcel valley (Aosta Region, Italian Western Alps).

Various mineralogical and geological studies have been carried out on the Praborna orebody since the beginning of this century (HUTTENLOCHER, 1934; DEBENEDETTI, 1965 and references therein). The more recent works were carried out by BONDI et al. (1978), BROWN et al. (1978), DAL PIAZ et al. (1979), MOTTANA et al. (1979), CASTELLO et al. (1980), GRIFFIN and MOTTANA (1982), MARTIN-VERNIZZI (1982), KIENAST and MARTIN (1983), MOTTANA (1986). The reasons for this interest are the presence of unusual metallic and silicate phases and the chance to study the effects of the low-T and high-P metamorphism on an unusual series of bulk compositions.

The purpose of this study is to describe the Praborna manganiferous deposit and its relationship with the surrounding ophiolites.

2. Geological setting

The metamorphic ophiolite units in the Western Alps, commonly known as the Piemontese Zone or as the Piemonte ophiolite nappe system include many Mn-deposits associated with quartzitic rocks and minor greenstones of the metasedimentary cover sequences (DEBENEDETTI, 1965; DAL PIAZ 1974a, 1974b; CHOPIN, 1978; DAL PIAZ et al. 1979; BEARTH and SCHWANDER, 1981; CASTELLO, 1981).

In the Aosta valley (Fig. 1) this composite nappe, tectonically sandwiched between the Upper Pennine Monte Rosa-Gran Paradiso nappes (Paleoeuropean margin) and the overlying Austroalpine Sesia-Lanzo and Dent Blanche s.l. nappe system (Paleoafrican/Apulian margin), marks the suture zone of the continental collision.

On the northern side of the middle Aosta valley and in the Valais the ophiolitic nappe system consists of the Zermatt-Saas and Combin main nappes and of many sheets derived from the closure of the oceanic segments and of the ocean-facing continental edges of the Jurassic Tethyan basin. These units record geochemical and lithostratigraphic differences related to distinct paleoenvironmental settings within the Tethyan ocean (BEARTH, 1964, 1967, 1973; DAL PIAZ, 1965, 1974a, 1974b, 1976; DAL PIAZ et al., 1972, 1979; KIENAST and TRIBOULET, 1972; KIENAST, 1973; CABY et al. 1978; DAL PIAZ and ERNST 1978; DAL PIAZ et al. 1981; BECCALUVA et al., 1984).

The Zermatt-Saas unit consists of oceanic-type ophiolite sequences overlain by a hetero-

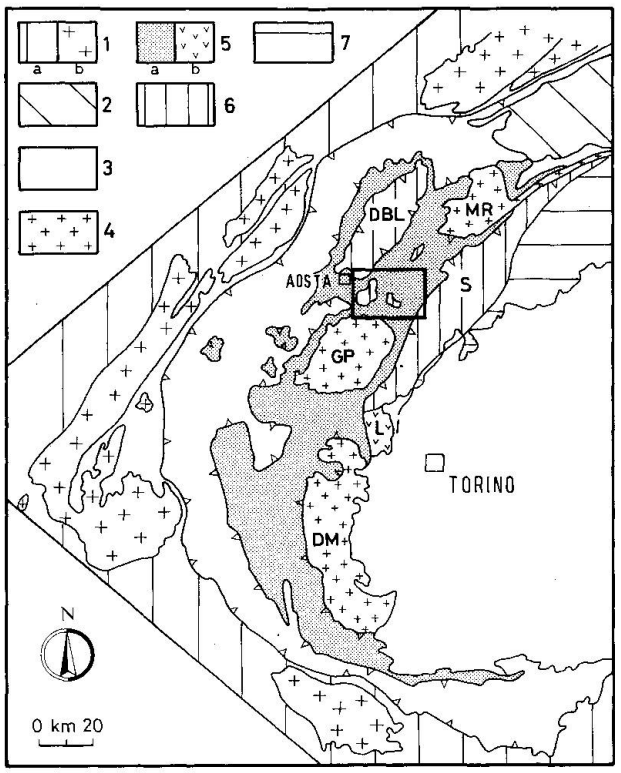

Fig. 1 Simplified map of the Western Alps showing the location of the St. Marcel valley and surrounding areas (the inset):
1) Helvetic cover (a) and basement (b) units; 2) Lower Pennine basement nappes; 3) Penninic Gran San Bernardo nappe including the Briançonnais cover, Subbriançonnais and Sion-Courmajeur units; 4) Penninic Monte Rosa (MR), Gran Paradiso (GP) and Dora Maira (DM) basement nappes; 5) Piemonte ophiolite nappe system (a), including the Lanzo Massif (b); 6) Austroalpine Sesia-Lanzo (S) and Dent Blanche (DBL) basement nappes; (7) Southern Alps.

geneous sedimentary cover. This latter sometimes exibits a volcano-sedimentary setting with marbles, calcschists, micaschists, quartzites and interbedded basaltic greenstones. Locally the post-volcanic cover shows a Ligurian affinity with basal Mn-Fe-rich metacherts followed by marbles and calcschists ("Scisti a Palombini" Auctorum).

The Praborna deposit is included in an ophiolite sequence occurring on the southern side of the Aosta valley, closely similar to the Zermatt-Saas unit. Both units are characterized by polyphase high-P, low-T early-Alpine metamorphism (Dal Piaz et al., 1972; Dal Piaz and Ernst, 1978; Ernst and Dal Piaz, 1978; Trümpy, 1980; Kienast, 1984), and by a heterogenous, locally pervasive, meso-Alpine greenschist facies overprinting.

In the St. Marcel, Savoney and Fenis valleys (Fig. 2) a thick section of the dismembered oceanic sequence is exposed. It comprises: - serpentinized peridotite tectonites, massive to layered metagabbros (Dal Piaz and Nervo, 1971); - glaucophane-rich metabasalts, overlying basal quartzites and pelite to carbonate metasediments (calcschists Auctorum).

In the St. Marcel valley the ophiolitic nappe mainly consists of metabasalts and calcschists with minor serpentinite and metagabbro slices (Figs. 3, 4). Metagabbro bodies, sometimes chromiferous, occur in the lower valley within basaltic glaucophanites. Glaucophanites grade upwards to coarse-grained garnet-chlorite-schists and talc-schists (i.e. at Fontillon, Servette) or to prasinites and chlorite-schists (i.e. at Praborna and at Mt. Corquet) including Cu-Fe($\pm$Zn) massive sulphide ores and disseminations. The overlying metasedimentary sequence is well exposed on the right side of the St. Marcel valley, between the Mt. Corquet and the Mt. Roux (Figs. 2, 4). Along the left side it is strongly deformed and tectonically overlain by mylonitic serpentinite slices and by the basement rocks of the Austroalpine Mt. Emilius Klippe (Figs. 2, 3).

The ophiolitic sequence, outcropping in the lower and middle St. Marcel valley, shows a complex fold interference pattern. Three main phases of deformation have been found: the earliest produced the eclogitic N-S trending, foliation and intrafolial F1 folds, deformed by 340-350 trending F2 folds. This F2 deformation, coeval with a blueschist facies retrograde overprinting (Tartarotti et al., in prep.), is mainly recorded in the glaucophanites/chlorite-schists complex outcropping in the lower St. Marcel valley (Fontillon, Servette).

The third deformation phase (F3), characterized by E-W trending axes of megascopic recumbent folds, postdates the HP metamorphism and appears to be connected with the partial retrogression of the blueschist assemblages into greenschist facies associations. Structures related to this deformation phase are well exposed on the right side of the St. Marcel valley (Mt. Corquet, P.ta Plan Ruè).

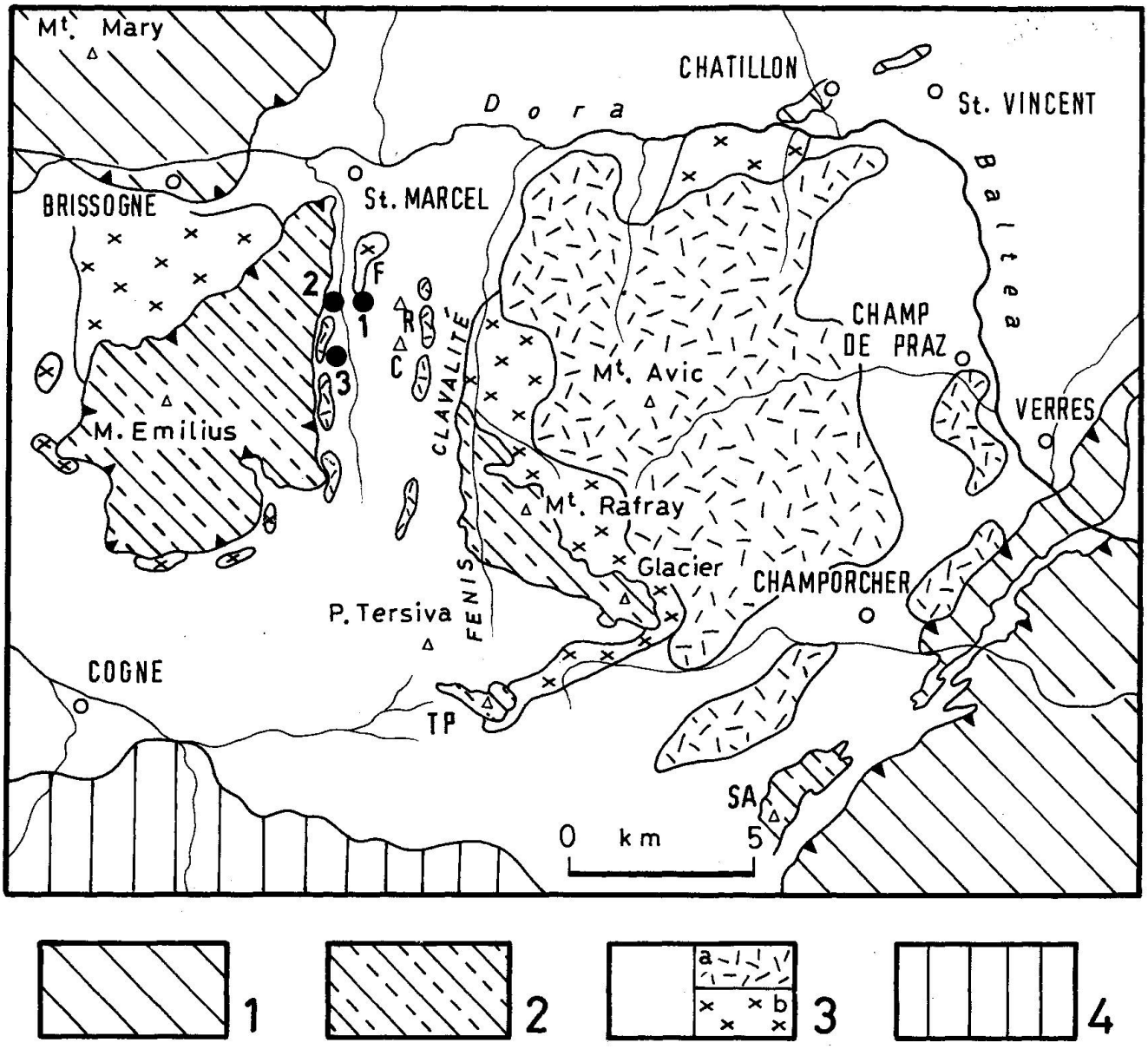

Fig. 2 Geological map of the right side of the middle Aosta valley. Austroalpine system: 1) Greenschist facies "Gneiss minuti" and Arolla complexes from the Sesia Lanzo and Dent Blanche nappes; 2) preserved and retrograded eclogitic micaschists of the Mt. Emilius, Glacier-Rafray, Tour Ponton and Santanel Klippen; 3) Piemonte ophiolite nappes system: undifferentiated calcschists and metaophiolite sequences, large serpentinized peridotites (a) and metagabbro bodies (b); 4) Penninic Gran Paradiso basement nappe:
1: Servette sulphide deposit; 2: Chuc sulphide deposit; 3: Praborna Mn ore; F: Fontillon; R: Mt. Roux; C: Mt. Corquet; TP: Tour Ponton; SA: Santanel.

3. Lithostratigraphy of the Praborna sequence

The manganiferous quartzites of Praborna are exposed on the left side of the middle St. Marcel valley (Fig. 2). They consist of banded quartzites and pyroxenites which include block lenses formed of massive braunite ± hausmannite or of fine grained braunite-quartz rocks (PERSEIL, 1985). The main manganiferous body (Fig. 5) appears on a front of fifty metres with a thickness ranging from 0.4 to 8 metres, and plunges to NW as exposed in the mine. The orebody is conformable with the schistosity of the surrounding quartzites.

The underlying section of the manganiferous quartzites and the lithostratigraphic sequence of Praborna are schematically represented in Figs. 4 and 5.

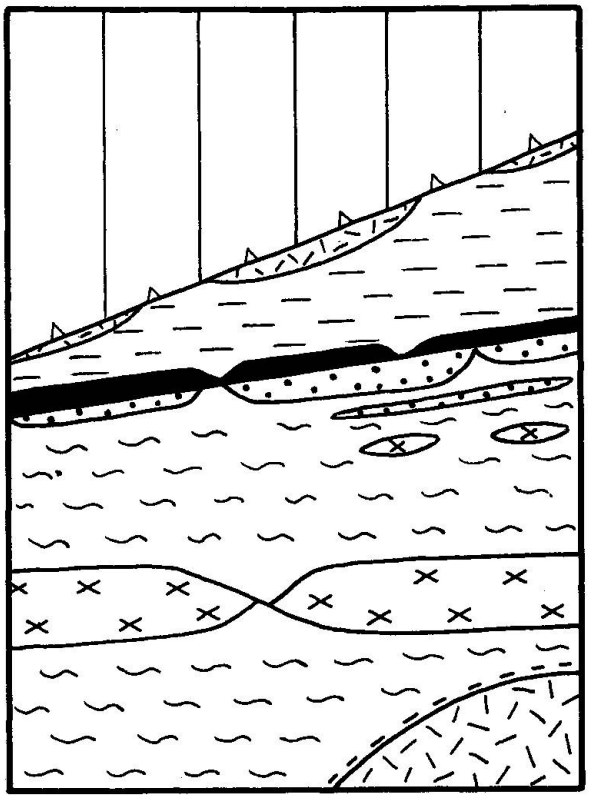

Fig. 3 Sketch of the lithologic sequence in the St. Marcel valley. a) serpentinized peridotite tectonites; b) metagabbro bodies; c) garnet-rich glaucophanitic metabasalts; d) chlorite-schists and prasinites; e) manganiferous quartzites; f) calcschists, marbles and associated micaschists; g) serpentinite mylonites; h) Austroalpine Mt. Emilius Klippe.

Laterally, the Mn orebody becomes much thinner and grades into banded quartzites and micaschists.

A thick section of metabasites overlies the Mn-sequence (its whole rock chemistry is reported in DAL PIAZ et al., 1978). These rocks are capped by sheared and strongly retrograded Cr-metagabbros, followed by repeatedly interbedded prasinites and calcschists.

Several generations of veins cut the quartzites, the massive Mn bodies and the overlying metabasites.

4. Petrography

Petrological studies have been developed on selected samples representative of the different levels and of the veins cutting the orebody. They show the existence of a first group of rocks with manganiferous assemblages connected with eclogitic foliation, intrafolial microfolds and with early fractures plus a second group connected with eclogitic foliation characterized by non manganiferous assemblages but becoming manganiferous successively, during late- and post-eclogitic fracturing.

Within the micaschists and quartzites capping the orebody some greenschist mineral phases increase their Mn content during Mesoalpine metamorphism and the late fracturing.

The eclogitic parageneses are exceptionally well preserved in the orebody, especially in the massive, slightly foliated pyroxenites, while, within the more foliated micaschists and within the glaucophanites underlying the orebody and in the overlying series, the eclogitic assemblages have been frequently transformed into greenschist facies.

The extensive presence of eclogitic parageneses in the orebody is probably due to its massive structure and moreover to its structural setting which is comparable with that of eclogitic pods preserved within retrograded metagabbros and glaucophanites of the St. Marcel valley. The field observations suggest that the orebody should represent the nucleous of a megascopic recumbent fold with axes E–W-trending, comparable with those described at the Mt. Corquet and Plan Ruè localities (TARTAROTTI et al., 1987).

A schematic description of the mineralogical assemblages observed in the main layers (Fig. 5) and then in the veins is given below.

4.1. MINERALOGY OF LAYERS

The major braunite ± hausmannite concentrations are included in a massive rock (level b, Fig. 5) constituted predominantly by aegirine-jadeite (Tab. 1; Fig. 6), minor quartz, albite, Mn-phengite and piemontite, already described by GRIFFIN and MOTTANA (1982), as well as by KIENAST and MARTIN (1983). The pyroxene porphyroclasts, roughly oriented according to eclogitic schistosity, are zoned and show a characteristic lack of Mn in the cores and a Mn increase in the more jadeitic rims (Fig. 7). The aegirine-jadeite crystals are crossed by microfractures filled by Mn-jadeite grains and successively by Mn-phengite (alurgite) and albite.

The aerigine-jadeite rocks are strictly associated with fine grained massive pyroxenites

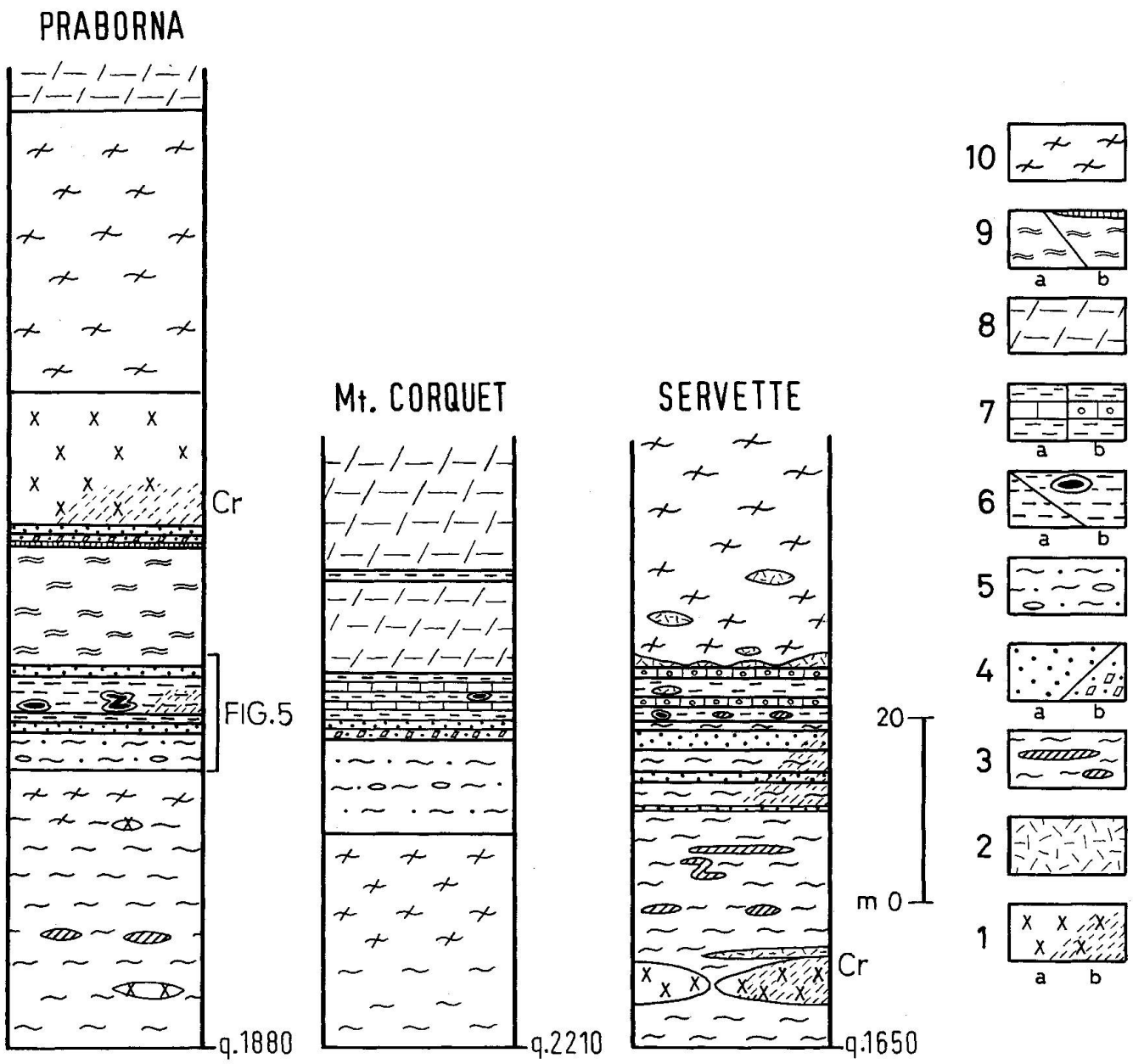

Fig. 4 Detailed sections of Praborna, Mt. Corquet and Servette ore bodies and related rocks. See Fig. 2 for their location.

1) Metagabbro bodies (a), sheared (b); often chromiferous (Cr) Mg-metagabbros.
2) Serpentinites.
3) Glaucophanites including centimetric to decimetric pods and bands of eclogite. At Praborna and at Mt. Corquet they appear more retrograded to garnet-amphibolites.
4) Chlorite-schists (a), locally with porphyroblasts of albite (b), probably derived from detrital basaltic material composition which suffered metasomatic transformation and shearing deformation.
5) Prasinites with centimetric chromiferous lenses and disseminated sulphides; they probably derive from gabbro detrital material.
6) Micaceous quarzites or micaschists often including pyroxene porphyroclasts and carbonatic lenses (a). They grade locally into manganiferous quartzites (b) including lenses of Mn-oxides and bands of Mn-silicates.
7) Silicate-bearing marbles (a) and garnet-pyroxene-fels (b).
8) Calcschists.
9) Fine-grained metabasites (a). At Praborna the metabasites of the top are metasomatically transformed into epidote-rich schists (b) in contact with overlying chlorite-actinote-bearing schists.
10) Retrograded glaucophanites and prasinites.

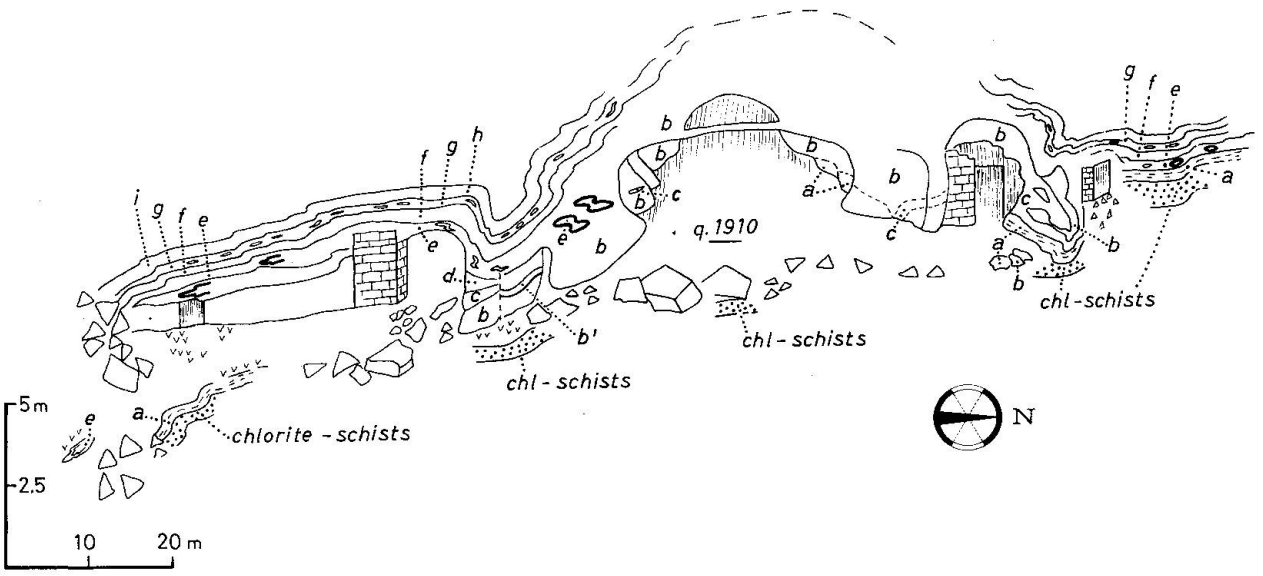

Fig. 5 Panorama of the Praborna mine:
a) quartzose micaschists locally including manganiferous lenses;
b) massive bed constituted by Mn-orebodies and associated aegirine-jadeite / chloromelanite-bearing pyroxenites;
b') piemontite-diopside-bearing quartzite grading into quartzose micaschists;
c) emerald green quartzite locally including chromiferous garnet clinopyroxene and hematite;
d) epidote-carbonate-clinopyroxene micaschists alternating with garnet-carbonate-hematite quartzites;
e) manganiferous zoned quartzites with typical lenses of braunite-garnet ± piemontite;
f) dark-green clinopyroxene-bearing rocks with garnet-quartzite;
g) pinkish boudinaged level including garnet-pyroxenoid-hematite assemblages;
h) tourmaline-bearing "ovardite" grading into fine grained metabasites cut by several generations of albite-hematite veins.

consisting of omphacite, chloromelanite, aegirine-augite pyroxenes (Fig. 8, Tab. 2), albite, quartz and minor piemontite. Also these rocks are brecciated and recemented by braunite, piemontite, albite, Mn-phengite, dark-purple Mn-omphacite (violan) and sodic augite which is sometimes manganiferous. The chloromelanite, which can grade to omphacitic compositions, or be overgrown by omphacite, is interpreted as a typical pyroxene of the early (prograde) high-P stage, by analogy with aegirine-jadeite (GRIFFIN and MOTTANA, 1982; MARTIN-VERNIZZI, 1982).

The Mn-omphacite and the Mn-jadeite are believed to have crystallized metasomatically at the peak of high-P metamorphism, following the mobilization of fluids induced by prograde reactions involving dehydration.

Locally (Fig. 5, level b'), the major braunite bodies grade into a reddish, fine-grained quartzite with predominant piemontite and minor (non manganiferous) diopside.

Micaschists (level d, Fig. 5) rich in carbonate, epidote and pyroxene overlie the piemontite-bearing quartzites. They are interbedded with more carbonatic layers, containing spessartine, tremolite, talc, hematite, rare piemontite and without braunite (Tab. 3).

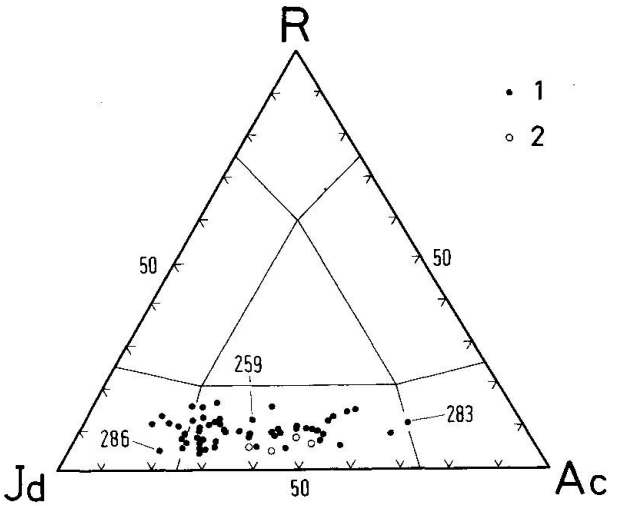

Fig. 6 Compositions of aegirine-jadeites from: 1) pyroxenites; 2) quartzites (fields after ESSENE and FYFE, 1967). Numbered dots refer to analyses listed in table 1.

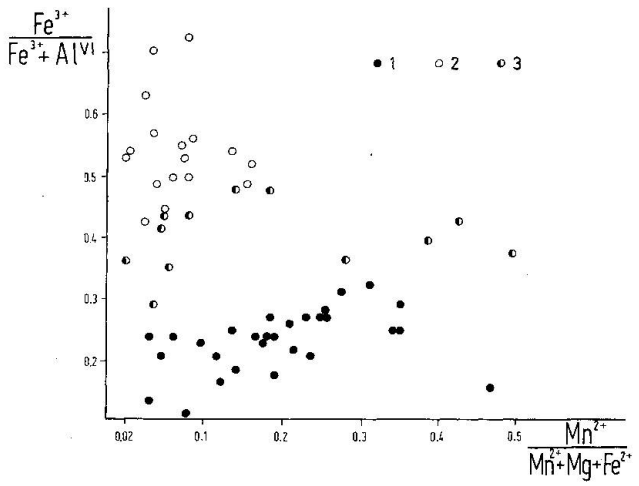

Fig. 7 Pyroxene distribution in terms of ratio: $Mn/(Mn + Mg + Fe^{2+})$ versus $Fe^{3+}/(Fe^{3+} + Al^{VI})$: 1) recrystallized purple jadeites; 2) pale-green aegirine-jadeite cores; 3) light purple aegirine-jadeite rims. $Mn_{tot} = Mn^{2+}$.

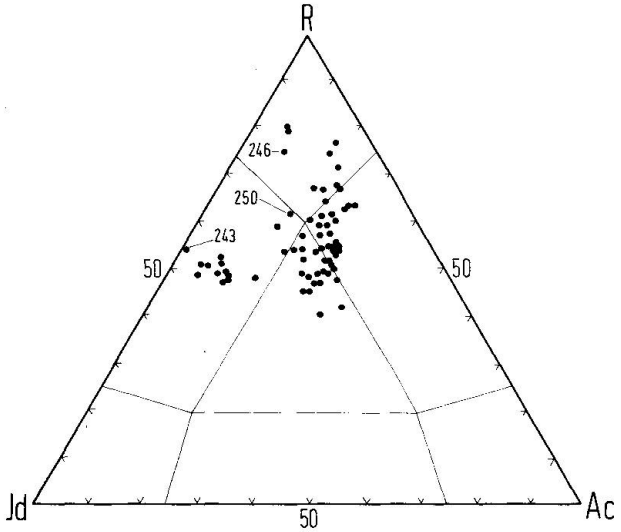

Fig. 8 Compositions of chloromelanite, dark-purple omphacite and sodic augite. Chloromelanite is interpreted as a typical pyroxene of early high-P stage, omphacite is believed to have formed later, at the peak of high-P metamorphism. The existence of a "solvus" between coexisting omphacite and augite was inferred by BROWN et al. (1978) and by CARPENTER (1980) but disproved by GRIFFIN and MOTTANA (1982).
All analyses are from one sample; numbered dots refer to analyses listed in table 2.

Laterally, a small fault connects them with an emerald-green feldspathic quartzite (level c, Fig. 5) including a clinopyroxene, the composition of which ranges from aegirine-augite to aegirine (Ac 45 to 80). This pyroxene is sometimes manganiferous (MnO up to 2%) and chromiferous (Fig. 9; Tab. 4). The less chromiferous aegirine-augite may be included within chromiferous garnet (Cr_2O_3 up to 15%; MERVEL pers. comm.) Cr-hematite (Cr_2O_3 up to

Tab. 1 Representative analyses of coexisting mineralogical phases from a aegirine-jadeite-bearing pyroxenite (sample 25-2).

	Jd	Aeg-jd	Aeg	Phe
	286	259	283	3
SiO2	57.50	56.10	55.10	52.09
TiO2	--	0.05	--	0.47
Al2O3	18.02	14.36	6.64	22.57
Fe2O3	--	--	--	1.95
FeO	6.34	11.42	21.99	--
MnO	1.60	1.49	0.24	1.23
MgO	0.95	1.28	1.58	5.07
CaO	1.16	1.87	1.85	0.03
Na2O	13.65	13.18	12.91	0.17
K2O	--	--	--	10.51
tot	99.22	99.75	100.31	94.09
Si	2.005	1.981	1.988	7.052
AlIV	--	0.019	0.012	0.948
AlVI	0.741	0.578	0.270	2.655
Ti	--	0.001	--	0.048
Fe3+	0.182	0.337	0.646	0.199
Fe2+	0.002	0.000	0.018	--
Mn2+	0.047	0.045	0.007	0.141
Mg	0.049	0.067	0.085	1.023
Ca	0.043	0.071	0.072	0.004
Na	0.989	0.902	0.903	0.045
K	--	--	--	1.815
tot	3.995	4.002	4.000	13.930

Tab. 2 Representative analyses from a chloromelanite-bearing pyroxenite (sample 25-3).

	Chlm	Omph	Aug	Fe-Omph	Amph
	158	243	246	250	
SiO2	54.37	57.15	55.11	54.51	58.41
TiO2	0.05	0.82	0.95	0.83	0.14
Al2O3	5.55	10.51	3.92	4.84	1.16
Fe2O3	--	--	--	--	--
FeO	9.36	1.77	3.45	6.93	1.15
MnO	0.77	1.16	1.18	0.97	0.32
MgO	8.95	9.07	12.34	9.54	23.43
CaO	12.65	14.04	18.97	15.16	11.28
Na2O	6.95	6.93	3.97	5.70	1.83
K2O	--	--	--	--	--
tot	98.86	101.45	99.89	98.52	97.95
Si	1.993	1.994	1.991	2.000	7.936
AlIV	0.007	0.006	0.009	0.000	0.064
AlVI	0.222	0.427	0.157	0.209	0.123
Ti	0.001	0.022	0.026	0.023	0.015
Fe3+	0.272	0.005	0.078	0.151	--
Fe2+	0.012	0.047	0.026	0.062	0.131
Mn2+tot	0.024	0.034	0.036	0.030	0.038
Mg	0.085	0.472	0.664	0.524	4.744
Ca	0.493	0.525	0.734	0.596	1.643
Na	0.490	0.469	0.278	0.405	0.483
K	--	--	--	--	0.040
tot	4.000	4.000	4.000	4.000	15.217

Tab. 3 Representative analyses of a carbonate-rich micaschist (sample 26).

	Gt			Mn-cc	Talc	Tr	Win
	33c	32 r m	35 r e				
SiO2	37.80	38.12	37.20	--	60.00	56.28	55.95
TiO2	--	--	--	--	--	0.08	--
Al2O3	20.59	20.41	19.99	--	0.07	0.84	1.15
FeO	3.21	15.54	3.34	--	0.47	4.73	7.27
MnO	28.68	16.75	30.64	10.28	0.35	4.06	3.74
MgO	0.58	0.51	0.47	2.18	29.48	20.84	20.22
CaO	8.64	10.34	7.11	40.14	0.16	8.88	7.07
Na2O	--	--	--	--	--	1.44	2.50
K2O	--	--	--	--	--	0.11	0.08
tot	99.50	101.67	98.75	52.60	90.53	97.26	97.98
Si	3.042	3.022	3.041	--	8.004	7.912	7.877
AlIV	--	--	--	--	--	0.088	0.123
AlVI	1.954	1.908	1.926	--	0.011	0.051	0.068
Ti	--	--	--	--	--	--	--
Fe3+	0.046	0.092	0.074	--	--	--	--
Fe2+	0.170	0.938	0.154	--	0.052	0.556	0.856
Mn2+tot	1.955	1.125	2.121	0.950	0.040	0.483	0.446
Mg	0.070	0.060	0.057	0.354	5.861	4.366	4.242
Ca	0.745	0.878	0.623	4.692	0.023	1.338	1.066
Na	--	--	--	--	--	0.392	0.685
K	--	--	--	--	--	0.197	0.014
tot	7.982	8.023	7.996	5.996	13.991	15.383	15.377

22: calculated on 22 oxygens .
45: tremolite overgrown on carbonate and talc;

Take is calculated on the basis of 22 oxygens.
Tremolite overgrown on carbonate and talc.
c = core; rm = middle rim; re = external rim

Tab. 4 Representative analyses from a chromiferous quartzite (sample 2c).

	Cpx		Hem		Gt	
	33 c	34 r	15	13	11	17
SiO2	53.77	54.47	0.44	--	36.00	35.99
TiO2	0.07	--	0.47	0.31	1.55	1.36
Al2O3	1.76	1.20	0.35	0.11	2.49	1.26
Fe2O3	--	--	91.58	97.99	--	--
Cr2O3	0.20	7.58	6.14	1.28	8.62	15.20
FeO	18.00	10.75	--	--	15.99	12.27
MnO	0.59	0.43	0.41	0.17	1.77	3.13
MgO	7.46	7.26	0.21	0.02	0.07	0.09
CaO	9.47	10.04	--	--	31.63	30.60
Na2O	8.64	7.94	0.18	--	--	--
tot	99.76	100.73	99.97	99.93	98.12	99.90
Si	1.970	2.009			3.028	3.004
AlIV	0.030	--			--	--
AlVI	0.046	0.052			0.247	0.123
Ti	0.002	--			0.098	0.085
Fe3+	0.552	0.295			1.012	0.770
Cr3+	0.006	0.221			0.573	1.003
Fe2+	--	0.037			--	--
Mn	0.019	0.013			0.126	0.221
Mg	0.407	0.399			0.008	0.011
Ca	0.372	0.397			2.850	2.736
Na	0.614	0.568			--	--
tot	4.018	3.991			7.942	7.953

Tab. 5 Representative analyses from a dark green quartzitic layer (sample 11).

	Chlm	Aeg-aug	Amph	Gt		Pyr
	60	70		7 c	9 r	
SiO2	55.27	53.38	58.11	37.83	37.02	0.20
TiO2	--	--	0.04	0.33	0.13	55.49
Al2O3	6.35	1.10	0.38	20.70	21.22	--
FeO	15.45	16.62	6.55	0.54	10.74	3.21
MnO	0.53	4.08	3.17	34.66	19.55	37.18
MgO	5.22	7.76	21.01	1.21	2.11	0.03
CaO	7.95	10.69	7.14	5.43	8.36	0.25
Na2O	9.73	7.12	2.87	--	--	--
K2O	--	--	0.11	--	--	--
tot	98.90	98.92	98.38	100.70	99.13	96.36
Si	1.987	1.966	8.000	3.033	2.973	0.010
AlIV	0.013	0.034	--	--	0.027	--
AlVI	0.256	0.014	0.062	1.956	1.983	--
Ti	--	--	0.004	0.020	0.008	2.116
Fe3+	0.436	0.511	0.448	0.037	0.003	--
Fe2+	0.028	--	0.306	--	0.718	0.136
Mn tot	0.016	0.127	0.369	2.353	1.330	1.597
Mg	0.280	0.426	4.105	0.145	0.253	0.002
Ca	0.306	0.422	1.053	0.466	0.719	0.014
Na	0.678	0.508	0.765	--	--	--
K	--	--	0.019	--	--	--
tot	4.000	4.009	15.130	8.010	8.014	3.875

Pyrophanite is calculated on the basis of 6 oxygens.

Tab. 6 Representative analyses from a rhodonite-garnet bearing rock (sample 343).

	Rhd	Gt	Hem	Pxm	Amph	Gt*	
	6			2		core	rim
SiO2	47.11	36.00	0.52	47.09	57.06	36.70	36.00
TiO2	--	0.92	0.16	--	0.02	0.33	0.41
Al2O3	0.01	16.71	0.01	--	0.19	16.64	12.43
Fe2O3	--	1.93	--	--	--	2.32	9.19
FeO	0.11	--	76.48	0.38	2.29	--	--
MnO	47.21	37.11	1.71	48.50	18.53	41.26	40.38
MgO	1.45	0.26	--	2.11	20.10	0.28	0.22
CaO	4.07	5.06	--	1.90	1.64	3.08	3.79
Na2O	0.01	--	--	--	0.58	--	--
tot	99.97	97.99	78.87	99.98	100.41	99.91	102.42
Si	2.005	3.035	0.035	2.007	7.984	3.017	3.009
AlIV	--	--	--	--	0.016	--	--
AlVI	--	1.661	0.001	--	0.015	1.644	1.225
Ti	--	0.058	0.008	0.002	--	0.021	0.026
Fe3+	--	0.122	3.877	--	--	0.146	0.578
Mn3+	--	0.159	--	--	--	0.189	0.171
Fe2+	0.004	--	--	0.014	0.268	--	--
Mn2+	1.702	2.491	0.098	1.751	2.196	2.740	2.688
Mg	0.092	0.033	--	0.134	4.192	0.035	0.027
Ca	0.186	0.457	--	0.087	0.246	0.277	0.339
Na	--	--	--	--	0.081	--	--
tot	3.991	8.016	4.019	3.993	15.076	8.069	8.063

Hematite is calculated on the basis of 6 oxygens.
* Garnet including oxide.

6%) and epidote are associated with the predominant pyroxenes.

The presence of chromiferous minerals such as clinopyroxene, garnet (reported also by COLOMBA, 1910) and hematite has been ascribed to the original presence of detrital Cr-minerals such as spinels and magmatic pyroxenes, or to the original presence of Cr-precipitates in the siliceous sediment (RONA, 1980). A polyphasic mobilization of chromium by circulating solutions during metamorphism is suggested by the crystallization of chromiferous rims on the large zoned pyroxenes and by the presence of Cr-muscovite (fuchsite) on the schistosity planes of some quartzites and in the fractures.

Over the green quartzites and the mica-schists there is an typical layer enclosing pods and folded lenses of spessartine bounded by braunite or, rarely, by piemontite (level e, Fig. 5).

Towards the top of the sequence dark-green massive rocks become predominant (level f). These consist of non-manganiferous chloromelanitic (Ac 50–60%; Fig. 10, Tab. 5) pyroxene often replaced by Mn-tremolite (with MnO up to 3%) or by brown manganiferous aegirine-augite. This latter pyroxene, characterized by MnO > 4%, possibly crystallizes at the expense of older chloromelanite and it is sometimes associated with spessartine, rutile and pyrophanite. Its composition is comparable with that of some late aegirine-augites which have been observed in the fractures of braunite pods as described by BONDI et al. (1978) and by GRIFFIN and MOTTANA (1982).

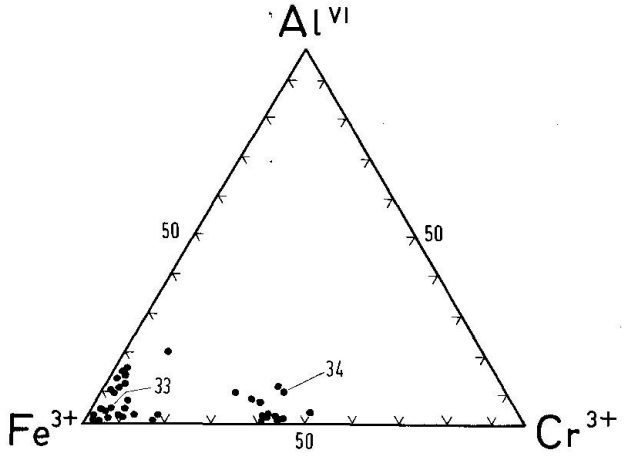

Fig. 9 Aegirine and chromiferous aegirine-augite in emerald-green quartzite. The Cr contents define a compositional gap between aegirine (Fe_{tot} = Fe^{3+}) and aegirine-augite (Fe_{tot} = Fe^{3+} + Fe^{2+}). The numbered dots refer to analyses listed in table 4. The analyses are from 4 samples.

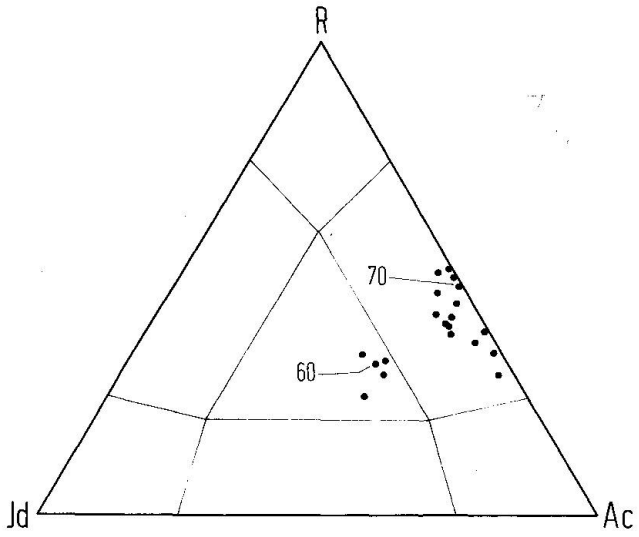

Fig. 10 Pyroxene composition from dark quartzitic bands; the recrystallized aegirine-augite contains MnO above 4%. The numbered dots refer to analyses listed in table 5. The analyses are from one sample.

Bands of Mn-garnet and kutnahorite are closely associated with the pyroxene-rich levels. Within the upper section of these a characteristic boudinaged horizon occurs (level g, Fig. 5). It is composed of quartz, yellowish spessartine, Mn–Fe-oxide, pyroxenoids and Mn–Mg amphibole (Tab. 6) with rare lenses of braunite, and it is cut by rhodochrosite veins.

Chlorite-albite schists rich in tourmaline are present at the top of the mineralized section (h, Fig. 5).

4.2. MINERALOGY OF VEINS

The veins and fractures crossing the Mn-ore bodies and the surrounding pyroxenites are very interesting because the assemblages record mostly high-P conditions.

A few of those observed are reported below:

a) quartz, rhodonite (fractures in the braunite bodies);

b) quartz, albite, manganiferous aegirine-augite, winchite, calcite (fracture in the braunite pods table 7);

c) quartz, albite, manganiferous omphacite and aegirine (quartz-bearing vein, table 8);

d) quartz, albite, calcite, sodic augite, K–Na

Tab. 7 Mineral phases from a fracture in the braunite orebody (sample 25-1).

	Win	Cpx	
SiO2	58.68	54.27	54.50
TiO2	--	--	--
Al2O3	0.62	0.83	0.74
FeO	6.36	12.44	24.72
MnO	0.43	3.56	0.59
MgO	20.61	9.06	3.86
CaO	5.05	11.81	5.18
Na2O	5.29	7.03	10.64
K2O	0.91	--	--
tot	97.95	99.00	100.23
Si	8.003	2.015	2.006
AlIV	--	--	--
AlVI	0.099	0.036	0.032
Ti	--	--	--
Fe3+	0.725	0.386	0.727
Fe2+	--	--	0.034
Mn	0.050	0.112	0.018
Mg	4.189	0.501	0.212
Ca	0.738	0.470	0.204
Na	1.399	0.506	0.759
K	0.158	--	--
tot	15.361	4.026	3.994

Tab. 8 Pyroxenes from a vein cutting a braunite pod (sample 19).

	Omph	Aeg
	1	2
SiO2	56.76	54.15
TiO2	0.58	0.15
Al2O3	10.69	1.25
FeO	5.67	24.94
MnO	2.74	1.00
MgO	6.29	2.85
CaO	7.77	3.54
Na2O	9.47	12.02
tot	99.97	99.90
Si	2.008	1.999
AlIV	--	0.001
AlVI	0.446	0.053
Ti	0.015	0.004
Fe3+	0.168	0.770
Fe2+	--	--
Mn	0.082	0.031
Mg	0.332	0.157
Ca	0.295	0.140
Na	0.649	0.860
tot	3.995	4.015

manganiferous amphiboles (quartz-bearing vein cutting braunite body, table 9);

e) quartz, albite, manganiferous omphacite and augite (fracture in the chloromelanite-bearing pyroxenite);

f) quartz, Mn-phengite, albite, piemontite, braunite (fracture in the chloromelanite-bearing pyroxenite, table 10).

In the described assemblages high-P parageneses prevail, while the re-equilibration in the greenschist facies is less pervasive. This re-equilibration is recorded particularly by the growth of albite-actinolite symplectite at the expense of the clinopyroxenes, and in general by a progressive hydration of the high-P parageneses.

In the Mn-bodies hausmannite also crystallized in the fractures of the braunite pods during the former (high-P climax) remobilization of Mn. During the later, but more pervasive circulation, braunite ± hausmannite are replaced by pyrolusite and then by cryptomelane (table 11; see PERSEIL and KIENAST, 1982 for a detailed description). The development of quartz-veins with albite-microline-Mn phlogopite-epidote-hematite in the aegirine-jadeite rocks is also ascribed to this event.

Centimetric veins of late generation containing quartz, piemontite and sometimes tremolite cross the piemontite-bearing quartzites, while veins filled with calcite or Mn-carbonate cross-cut the garnet-pyroxenoids rocks and the carbonate-bearing micaschists.

Tab. 9 Representative analyses from a quartz-bearing vein cutting the Mn-body (sample 4/82).

	Ca-amph	K-Rt		Cpx	Cc
		core	rim		
SiO2	58.39	57.02	58.02	55.50	0.74
TiO2	0.10	0.22	0.07	0.07	0.10
Al2O3	0.10	0.60	0.34	0.59	--
FeO	2.66	2.41	2.77	3.14	0.30
MnO	0.34	1.60	0.38	0.55	--
MgO	22.65	21.34	23.27	15.47	0.25
CaO	8.04	4.86	10.26	22.63	56.41
Na2O	3.99	6.32	2.38	1.69	--
K2O3	1.70	3.08	0.47	--	--
tot	97.97	97.45	97.96	99.64	57.81
Si	8.000	8.000	7.958	2.013	0.071
AlIV	--	--	0.042	--	--
AlVI	0.016	0.099	0.013	0.025	--
Ti	0.011	0.023	0.007	0.002	0.007
Fe3+	0.243	0.126	--	0.090	--
Fe2+	0.062	0.150	0.318	0.005	0.024
Mn	0.039	0.188	0.050	0.017	--
Mg	4.626	4.422	4.756	0.836	0.036
Ca	1.180	0.724	1.508	0.880	5.784
Na	1.060	1.703	0.633	0.119	--
K	0.297	0.547	0.082	--	--
tot	15.534	15.982	15.367	3.987	5.922

Tab. 10 Representative analyses of silicate phases from a fracture crosscutting a chloromelanite-bearing pyroxenite (sample 25-3).

	Phe		Pm	Phl
	16	27	1	
SiO2	50.60	55.99	38.09	41.71
TiO2	1.14	0.18	0.56	0.96
Al2O3	22.19	19.40	20.08	15.68
Fe2O3	2.65	0.33	1.94	2.34
FeO	--	--	--	--
MnO	1.22	2.28	15.46	3.79
MgO	6.76	6.31	0.48	19.81
CaO	0.13	0.09	21.44	0.22
Na2O	0.58	0.35	0.14	0.51
K2O	10.29	10.88	0.19	10.16
tot	95.66	95.81	98.38	95.18
Si	6.811	7.453	3.024	5.977
AlIV	1.189	0.547	--	2.023
AlVI	2.326	2.490	1.879	0.564
Ti	0.116	0.018	0.035	0.102
Fe3+	0.269	0.033	0.117	0.246
Fe2+	--	--	--	--
Mn2+tot	0.139	0.257	1.039	0.450
Mg	1.354	1.250	0.006	4.132
Ca	0.020	0.014	1.825	0.034
Na	0.151	0.090	--	0.139
K	1.765	1.843	--	1.814
tot	14.140	13.995	7.925	15.481

16: brownish phengite grown as lamella in the cleavage of alurgite

5. Mineral compositions

A variety of mineral analyses were selected to document the compositional range of each mineral; tables have already schematically shown the composition of a few minerals from individual representative samples. The chemical analyses were performed by microprobe; procedures and results were reported extensively by MARTIN-VERNIZZI (1982). We would like here to add that:

i) pyroxene and pyroxenoid analyses were recalculated by the PAPIKE et al. (1974) method which gives a balanced charge over four cations and the terminology of ESSENE and FYFE (1967) was used. For illustrative purposes, the following end-members were calculated sequentially: $NaFeSi_2O_6$, $NaAlSi_2O_6$, $CaTiAl_2O_6$, $CaFe(AlSi)O_6$, $CaAl(AlSi)O_6$, $Ca_2Si_2O_6$, $Mg_2Si_2O_6$, $Fe_2Si_2O_6$.

ii) Amphibole analyses were also calculated using the PAPIKE et al. (1974) method; the nomenclature proposed by the I.M.A. (LEAKE, 1978) was adopted.

iii) Epidote group minerals were calculated on the basis of 12.5 oxygens; all iron was attributed to Fe^{3+}, Mn was allotted as Mn^{3+} in sufficient amount to make up any deficiency in: $Al + Fe^{3+} = 3$ with the remainder of the manganese allotted as Mn^{2+}.

iv) Garnets were calculated on the basis of 12 oxygens and Fe^{3+} was estimated reducing the cation sums to 8; iron was allotted as Fe^{3+} in sufficient quantity to make up any deficiency in $Al + Cr + Ti = 2$ the remainder of the iron is allotted as Fe^{2+}. For those garnets which have a cation deficiency after conversion of Fe^{2+} to Fe^{3+}, Mn^{2+} was oxidized to Mn^{3+}.

v) Mn-white mica and Mn-phlogopite analyses were calculated on the basis of 22 oxygens and all iron was assumed to be ferric, as suggested by the ubiquitous presence of braunite and hematite.

Clinopyroxenes: The composition of clinopyroxene in the Praborna rocks has a wide range (Fig. 11). The occurrence of the coexisting omphacite and augite, jadeite and aegirine in individual samples has been shown in the

Tab. 11 Representative analyses of Mn-oxides.

	sample 25-2			sample 25-3		
	Brn	Prs	Krp	Brn	Brn	
SiO2	9.93	4.59	0.05	10.05	10.35	10.54
TiO2	--	0.67	--	0.03	1.09	3.82
Al2O3	0.23	0.51	0.79	0.25	0.32	0.03
Fe2O3	0.35	0.86	0.85	0.95	1.86	6.43
MnO	81.22	64.07	70.69	80.49	77.02	65.68
MgO	0.63	0.13	0.03	0.73	0.18	0.13
CaO	0.60	2.65	--	0.70	1.57	4.32
Na2O	0.01	0.08	0.02	--	--	--
K2O	0.03	2.59	3.64	--	--	--
tot	93.00	76.15	76.07	93.20	92.39	90.95

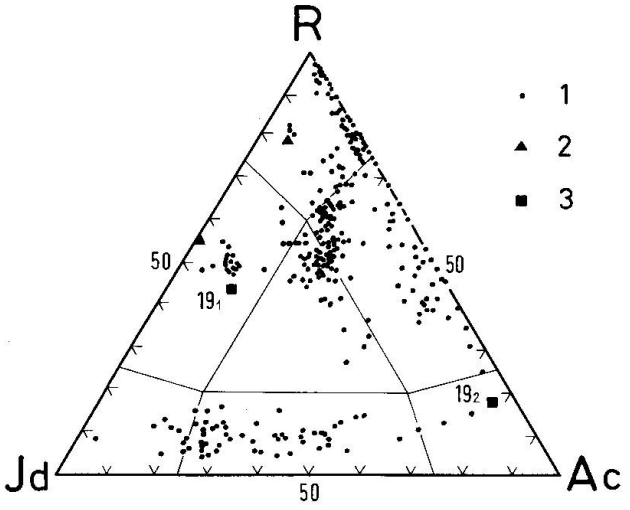

Fig. 11 Pyroxenes from veins and massive rocks (1). Two examples of coexisting pyroxenes in veins are reported here: from a vein which cuts the chloromelanite pyroxenite (2); from a vein which cuts a braunite-hausmannite pod (3). The numbered dots refer to analyses listed in table 8.

previous diagrams (Figs. 6, 8), while the coexistence of omphacite and jadeite has been documented by GRIFFIN and MOTTANA (1982).

Discussion of the omphacite-jadeite and sodic augite-omphacite miscibility gaps and of the solid solutions between aegirine and jadeite or aegirine and cosmochlore are reported by BROWN et al. (1978), CARPENTER (1980), GRIFFIN and MOTTANA (1982), KIENAST and MARTIN (1983), ABS-WURMBACH et al. (1984) and MOTTANA (1986). Figure 11 only gives the evidence for the observed compositional gaps which indicate that clinopyroxenes appear to be either strongly sensitive to bulk composition of host rock of to the chemistry of metasomatic solutions circulating in the fractures and in the veins.

Pyroxenoids: The existence of two pyroxenoid types (rhodonite and possible pyroxmangite), characterized by variable Ca content is shown in the (Fe^{2+} + Mg)-Mn-Ca diagram (Fig. 12, Tab. 6). In the same sample (Pr 343) the relatively Ca-rich member (Ca up to 10%) is associated in apparent equilibrium with manganiferous garnet and Mn-hematite, while the Ca-poor member is associated with a Mn–Mg rich amphibole.

Garnets: Garnets represented in figure 13 belong to quartzitic levels interbedded with pyroxene-rich layers (Tab. 5) and to carbonate-rich micaschists (Tab. 3), both being braunite-free. Their spessartine contents vary from 40% to 80%; the cores and the external rims show the highest content of MnO.

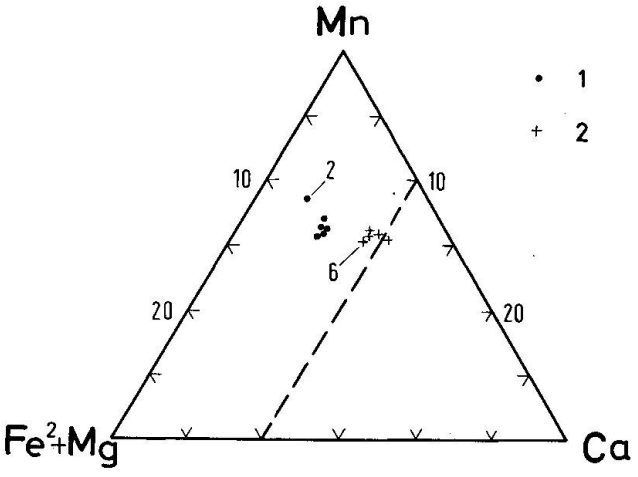

Fig. 12 Pyroxenoid compositions: 1) pyroxenoid associated with Mn–Mg rich amphibole; 2) pyroxenoid associated with garnet. The analyses are from one sample only; the numbered dots refer to those reported in table 6.

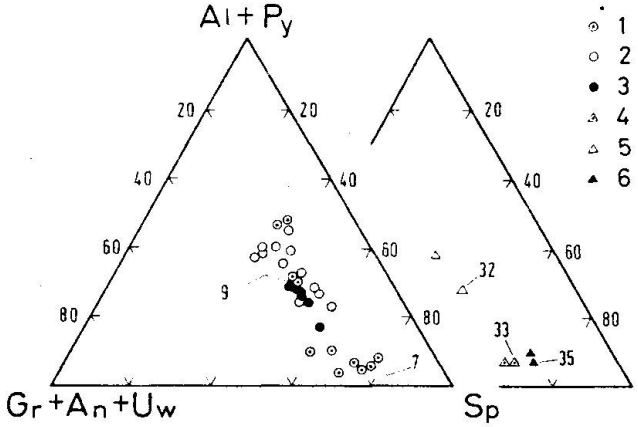

Fig. 13 Garnets from a pyroxene-garnet quartzite: 1) core, 2) internal rim, 3) external rim; from a carbonate-rich micaschist: 4) core, 5) internal rim, 6) external rim. The numbered dots refer to analyses listed in tables 5 and 3.

In the pyroxenoids-garnet-rich quartzite the garnet closely associated with rhodonite appear to be very rich in manganese and poor of iron (Fe_2O_3 = 1.93, Tab. 6), while the garnets from a level lacking pyroxenoids are richer in iron (Fe_2O_3 = 2.32 to 9.19%). The lack of braunite and of other manganiferous oxidized phases in this assemblage probably produced a Mn^{3+} bearing-garnet (with the blythite, $Mn_3^{2+}Mn_2^{3+}[SiO_4]_3$, end-member). The rhodonite-Fe-oxide association prevented the crystallization of Fe-Mn-bearing garnet (with the calderite, $Mn_3^{2+}Fe_2^{3+}[SiO_4]_3$, end-member) according to the experimental studies of LATTARD and SCHREYER (1983).

Almandine garnets have been identified in a quartzitic level interbedded with epidote-aegirine-augite quartzite; their rims show a slight enrichment in MnO.

Piemontite and epidote: Piemontite occurs in quartzites, braunite pods and pyroxenitic rocks as small grains, and in the veins as beautiful centrimetric crystals. In the quartzites they are generally homogeneous and contain Pm 27 (Pm = $Ca_2Mn_3^{3+}Si_3O_{12}(OH)$) to 33, while in chloromelanitic rocks they are zoned with Pm 30–40 and Ps (Ps = $Ca_2Fe_3^{3+}Si_3O_{12}(OH)$) ranging from 20% in the core to 5% in the rims (Fig. 14).

In the quartz-albite veins of the later generation which cross the orebody, the piemontites are characterized by 43% of Mn^{3+} substitution for Al^{3+} (MOTTANA and GRIFFIN, 1983). But in the veins cutting the aegirine-jadeite rocks the

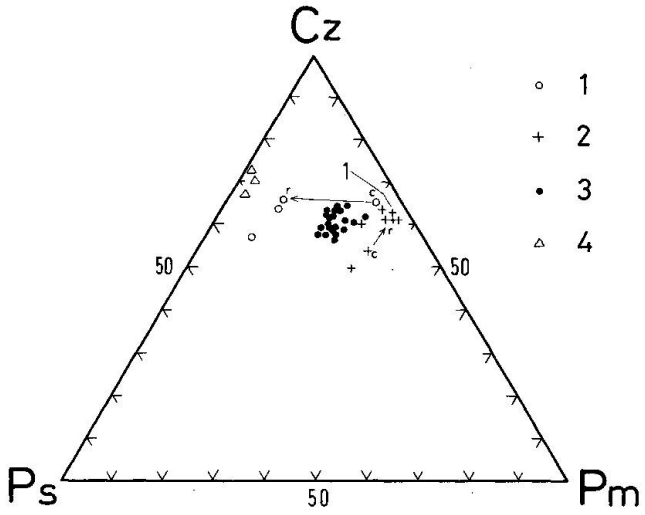

Fig. 14 Piemontite and epidote compositional variations from the Praborna rocks: 1) piemontite from the veins which cut the aegirine-jadeite rocks; 2) piemontite from the chloromelanite rocks; 3) piemontite from the braunite-bearing quartzites; 4) epidotes from the micaschists and aegirine-augite-bearing micaschists and aegirine-augite-bearing quartzites. The numbered dot refers to analysis listed in table 10. Definitions of coordinates: see text.

rare piemontite shows an interesting increase of Ps end-member in the rims (Pm 35, Ps 5 to Pm 10 Ps 23) and true pistacite may also crystallize (Fig. 14).

Besides piemontite, epidote (Ps 20–40, Pm 5%) is an important phase in the Praborna micaschists and in the pyroxene-bearing quartzites. In these rocks it seems to develop at the expense of pre-existing pyroxenes. In some Fe-rich rocks, closely associated with manganiferous concentrations, the epidotes show pink patches and rims due to the presence of Mn^{3+}. This feature as well as the local presence of minute braunite crystals, suggests the oxidation of the system during the late circulation of fluids.

Phengites: In the manganiferous layers the phengites exhibit a characteristic pink pleochroism due to octahedral manganese (RICHARDSON, 1975). The micas are generally slightly green or colorless in the other schists. Both range from true phengites with a high content of Si in the tetrahedral site (Si 3.6–3.5) to more muscovitic types with lower Si (Si 3.4; Tab. 10).

Moreover it is interesting to note that in fractures crossing the manganiferous pods, the pink phengites crystallize with an appreciable paragonite content (Fig. 15), due to the chemistry of the solutions circulating during the late/post eclogitic stage. They sometimes include omphacite and piemontite in the chloromelanite, aegirine-jadeite-bearing rocks.

Phlogopite: This phase appears to crystallize at the expense of pink phengites and of piemontites in connection with late metasomatic processes. Its high content of MnO (Tab. 10) is closely related to the composition of the pre-existing manganiferous phases or to that of the minerals with which it is in contact.

The Mn-phlogopites, already described by BROWN et al. (1978), show a characteristic red-brown pleochroism due to titanium TiO_2 up to 1.33%) and iron (Fe_{tot} = Fe_2O_3 up to 6%) contents.

Mn-oxides: In the Praborna orebodies braunite is the most important Mn-oxide. It forms monomineralic recrystallized concentrations with characteristic mosaic structure. These are surrounded by fine-grained aggregates of late-developped braunite and quartz (PERSEIL, 1985).

Major contents of Fe, Ca, Ti and a decrease in Si and Mn characterize the second braunite generation. This braunite is sometimes associated with hausmannite, and both result from the circulation of Mn-bearing solutions during the high-P event, synchronous with the crystallization of Mn-omphacite and Mn-phengite.

The transformation of braunite into more hydrated and oxidized phases, such as pyrolusite, and into phases enriched in K_2O as cryptomelane (Tab. 11) is important along the frac-

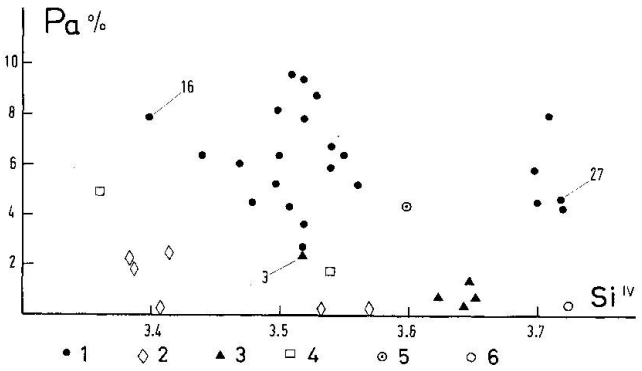

Fig. 15 Paragonite and Si atom contents p.u.f. in the phengites. 1) micas from chloromelanite-bearing pyroxenite and related veins; 2) from a phengite-rich quartzite; 3) aegirine-jadeite-bearing pyroxenite; 4) from a micaschist; 5) mica analysis after PENFIELD (1893); 6) after BROWN et al. (1978). The numbered dots refer to analyses listed in tables 1 and 10.

tures and is coeval with the development of Mn-phlogopite and microcline. The presence of braunite in the mineral assemblages plays a dominant role in the chemistry and the stability of the silicate phases, independent of P and T conditions. In fact, only silicates lacking Fe^{2+}, such as feldspars, sphene and Fe-free carbonates and oxidized phases such as Mn-phengite ($Fe_{tot} = Fe^{3+}$), Mn-Phlogopite ($Fe_{tot} = Fe^{3+}$), piemontite and epidote are in equilibrium with braunite. Garnet is stable only when it is almandine-free.

Braunite coexists with different types of amphiboles: with slightly manganiferous richterite and winchite, both crystallized in the fractures of the Mn pods, and with tremolite and actinote, both common in the quartzites and in the late veins. In the braunite-free veins tremolites may contain greater amounts of MnO, while pink phengite, phlogopite, piemontite and pyroxenes generally have a higher content of MnO when they are in contact with braunite.

Amphiboles: According to the I.M.A. classification (LEAKE, 1978) most of the analyzed amphiboles from quartz-albite-piemontite veins are tremolites, sometimes manganiferous (MnO up to 4%), and actinolites. Among those examined from mineralized samples only the amphiboles from the veins crossing braunite pods have the composition of richterite of winchite (Tab. 7-9). The first analyses of these amphiboles were carried out by RONDOLINO (1936); recently potassium-fluorrichterites have been described by MOTTANA and GRIFFIN (1985) in a quartz-rich rock from Praborna.

6. Oxygen fugacity in the ore body during alpine metamorphism

The Praborna manganiferous sequence shows a compositional banding produced by the distribution of Fe-silicates (Fe-epidote, Fe-clinopyroxene, Fe-garnet), Mn-silicates (piemontite, spessartine, Mn-clinopyroxene) and Mn-oxides.

This compositional banding is assumed to reflect a primary depositional sequence with differences in chemical composition and state of oxidation.

The occurrence of thin braunite-free bands alternating with piemontite-braunite layers indicates that oxygen activity was controlled by the original chemistry, and little, if at all, by metamorphism.

In general, the Praborna sequence shows a fO_2 higher than that found in surrounding metabasalts, which are characterized by fO_2 below the hematite-magnetite buffer as indicated by the presence of dispersed magnetite and pyrite.

The occurrence of braunite in many Mn-rich metamorphic assemblages developed during the high-P and greenschist events, shows that the fO_2 changed only slightly. However, manganese may have occurred as oxides of a higher valence state in the sediments before metamorphism. During hydrothermal deposition Mn probably precipitated as $Mn(OH)_4$ and MnO_2 (EDMOND et al., 1979, SIVAPRAKASH, 1980), which later recrystallized into pyrolusite and cryptomelane. During the lithification and the earliest metamorphic events, reactions such as 7 pyrolusite + SiO_2 = braunite + 2 O_2 (HÜBNER, 1967; ABS-WURMBACH et al., 1983) transformed these high valency oxides (4+) into a relatively lower valency state (3+, 2+). Subsequently fO_2 did not change much and remained above 10^{-10} as demonstrated by the coexistence of braunite + hausmannite or hausmannite + rhodonite during alpine metamorphism.

In the Praborna quartzites the following types of metamorphic parageneses in relation to different fO_2 conditions are recognized (Fig. 16):

A) manganiferous, with braunite;
B) manganiferous and ferric, braunite-free, with hematite;
C) ferrous, hematite-free.

The typical manganiferous assemblages including braunite are:

A1) quartz + braunite;
A2) quartz + braunite + piemontite;
A3) quartz + braunite + spessartine;
A4) quartz + braunite + piemontite + spessartine;
A5) quartz + braunite + rhodonite.

In these assemblages, characterizing the most oxidized layers, partridgeite $(Mn,Fe)_2O_3$ associated with braunite has never been observed; thus the above assemblages have fO_2 below that defined by the partridgeite-hausmannite buffer.

The coexistence of braunite with rhodonite (or pyroxmangite) and quartz (2 braunite + 12 quartz = 14 rhodonite + 3 O_2; ABS-WURMBACH et al., 1983) has been observed in the fractures

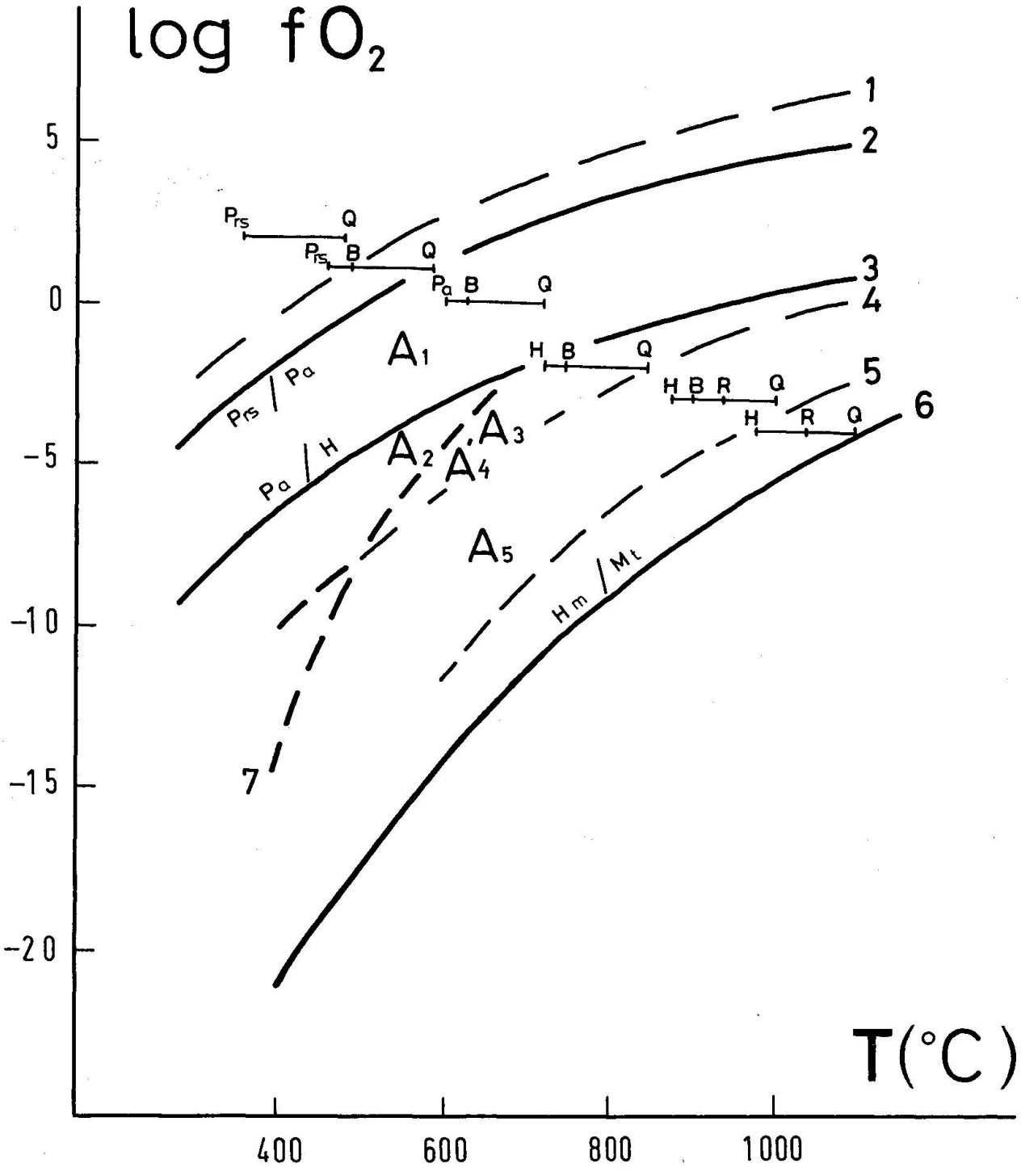

Fig. 16 Approximate positions of manganiferous parageneses of Praborna for P = 15 kb and for a T range in accordance with the eclogitic metamorphism (after ABS-WURMBACH et al., 1983).
Reaction curves: 1) 7 pyrolusite + 1 quartz (cristobalite) = 1 braunite + 2 O_2 ; 4) 2 braunite + 12 quartz (cristobalite) = 14 rhodonite (pyroxmangite) + 3 O_2; 5) 2 braunite = 4 hausmannite + 2 rhodonite (pyroxmangite) + O_2; 7) piemontite = spessartine + ¼ H_2O + ¼ O_2 calculated for Pf = 15 kbar from the data of V, T and fO_2 given by KESKINEN and LIOU (1979) for Pf = 2 kbar. The variations of fH_2O from 2 kbar to 15 kbar have been calculated from the data of BURNHAM et al. (1969) and of DELANY and HELGELSON (1978).
Buffer curves: 2) pyrolusite-partridgeite, 3) partridgeite-hausmannite, calculated from the data of HÜBNER and SATO (1970) for P = 15 kbar; 6) hematite-magnetite from the data of EUGSTER and WONES (1962).
Manganiferous assemblages including braunite: A1) Q-B; A2) Q-B-Pm; A3) Q-B-Sp; A4) Q-B-Pm-Sp; A5) Q-B-R.

cutting the main oxide bodies. The assemblage defines relatively low fO_2, presumably near the low fO_2 end of the braunite stability range (ABS-WURMBACH, 1980). In the samples analyzed the rhodonite-braunite-quartz assemblage shows textural features indicative of equilibrium on the univariant curve calculated by MUAN (1959).

Similarly in a fracture of the main braunite bodies, coexisting braunite and hausmannite have been recognized, as inclusions in the diopside which replaces, with albite, the high-P pyroxenes.

The manganiferous parageneses including hematite are:

B1) quartz-piemonte-spessartine;
B2) quartz-rhodonite-spessartine;
B3) quartz-aegirine-augite-spessartine-pyrophanite;
B4) quartz-epidote-garnet, or quartz-epidote- carbonate.

These are characterized by a slightly variable oxidation state dependent on silicate phases. According to KESKINEN and LIOU (1979) and BROWN et al. (1978) the piemontite-garnet association indicates fO_2 above 10^{-20}, which is comparable to the fO_2 recorded by braunite-quartz.

The B2), B3) and B4) assemblages indicate a low fO_2 (LIOU, 1973).

The hematite-free parageneses frequently include Fe-epidote or garnet and carbonate and indicate a low fO_2. The oxidation state of these last types of rocks is comparable to that of the surrounding metabasalts.

The ferrous parageneses described show a characteristic late enrichment of manganese and a possible oxidation which is indicated by pink rims and spots in the epidotes s.s. and carbonates.

7. Discussion: Geological environment of Praborna and of associated Cu-Fe sulphide deposits.

The widespread presence in the St. Marcel valley of chlorite-schists and talc-schists in the upper part of the metavolcanic sequence is worthy to note.

These have been interpreted as deriving from basaltic material of detrital origin (pillow-lavas, hyaloclastites and/or basaltic sandstones) strongly affected by the oceanic hydrothermal alteration (BONATTI, 1975; 1981; EDMOND et al., 1979; CASTELLO et al., 1980; RISE PROJECT GROUP, 1980; MOORBY et al., 1983; MOTTL, 1983; CONVERSE et al., 1984) and by lower-T basalt-sea-water interaction (ALT and HONNOREZ, 1984), as suggested by the peculiar composition and by high content of MgO (9–11%; discussion in DAL PIAZ et al., 1981).

Furthermore the strong relationship existing among the Mg-metasomatism which involved this basaltic material, the development of sulphide-ores (Servette-Chuc) and the presence of manganiferous quartzites confirm the above mentioned hydrothermal events. Besides at Praborna sulphides occur as disseminated deposits in the underlying prasinites and chlorite-schists while Fe-silicates ± hematite are widespread within the quartzites and mica-schists surrounding the manganiferous bodies.

The structure and mineralogy of the Praborna quartzites and the geological context suggest that the original sequence was probably similar to present day metalliferous sediments s.l. of hydrothermal origin, which may include ferruginous, Mn-poor oxy-hydroxide deposits and more oxidized concentrations of massive Mn-ore. The Praborna quartzites, rich in Mn and Fe minerals, could be considered as resulting from similar-ochre deposits (ROBERTSON and HUDSON, 1974) developed by precipitation of Fe and minor Mn from hydrothermal solutions debouching onto the sea-floor at the sediment-seawater interface (BONATTI, 1975; MOORBY et al., 1983).

Usually the ochres show a lateral or vertical transition into more oxidized and manganiferous members ("umbers"). This transition is attributed to local and extreme fractionation of Mn from Fe.

The sulphides generally associated with the manganiferous deposits may be considered as the earliest members of hydrothermal fractionation (CRONAN, 1980). These were formed during the ascent of hydrothermal solutions into the upper oceanic crust, when the chemical conditions were still reducing (BONATTI et al., 1976; RONA et al., 1976; EDMOND et al., 1982).

In deposits of the Western Alps similar to those observed in the St. Marcel valley, according to DAL PIAZ et al. (1978), and MARTIN and POLINO (1984) most silica have been interpreted as being of hydrothermal origin and only slightly biogenic.

8. Metallogenesis and metamorphic evolution in the St. Marcel Rocks

8.1. OCEANIC METAMORPHISM

Oceanic metamorphism was linked to hydrothermal activity, thus it produced metasomatic transformations of the original basalts and of the first sediments. During the ascent of hydrothermal solutions the following succession of events probably took places:

a) sulphide deposition as massive bodies, as stockwork-type veinlets and as disseminations within the middle and upper section of the basaltic sequence, under reducing conditions.

b) General enrichment in Mg, Al, Si, (Na,Ca) in the basaltic rocks at the seawater-basalt interface. The lack of Mn-sulphide in the St. Marcel deposits indicates that no Mn was added to rocks during this stage. This may be due to the inverse relationship between H_2S and Mn (EDMOND et al., 1979) in the debouching hydrothermal solutions. The deposition of sulphides was closely connected with the hydrothermal silica precipitation as indicated by the abundant presence of sulphide within the quartzitic layers and lenses of the metasedimentary cover (Chuc sulphide deposit).

c) Fe-oxy-hydroxide fractionation and Mn minor accumulation in the first sediments overlying the basaltic crust. During this stage, part of the primary sulphides may have been also oxidized by reaction with oxygenated seawater.

The Fe-Mn minerals association appears to be most common on the ocean floor, where it forms the basal deposit in the sedimentary column (DYMOND et al., 1973). This type of metalliferous deposit is also very common in the Western Alps and in the Apennines, but it never attains any great dimensions.

d) Local deposition of Mn muds in very oxidizing conditions.

e) First mobilization of Mn and Fe within the sedimentary pile during diagenesis.

8.2. HIGH-PRESSURE POLYPHASE METAMORPHISM

The following high-P metamorphism related to Alpine subduction is characterized by several stages. P probably ranged from 8 to above 10 kbar in the St. Marcel ophiolites (MOTTANA, 1986 suggests P ranging up to 14 kbar in the eclogitic conditions) and in the Mt. Emilius Klippe (ERNST and DAL PIAZ, 1978; DAL PIAZ et al., 1983). T ranged from about 300 °C defined by the pre-eclogitic lawsonite and aragonite stability (BROWN et al., 1978) to 550 °C, defined by the Fe-chloritoid breakdown (GANGULY, 1969).

During the prograde evolution, feldspar, epidote, chlorite, white mica and amphiboles formed in the oceanic environment reequilibrated, while other minerals developed from preexisting phases. At Praborna the aegirine-jadeite and chloromelanite pyroxenes may be supposed to have crystallized from ophiolite debris (magmatic pyroxenes); spessartine, piemontite, pyroxenoids and Mn-oxides crystallized in the manganiferous layers from preexisting Mn-minerals. Aragonite, Ca–Na amphiboles and certain clinopyroxenes developed in the early fractures created within the sequence during the previous stage. Lawsonite, Na–Ca-amphiboles, chloritoid and garnet crystallized in the surrounding metabasalts.
During this prograde path towards the eclogitic climax, the minerals become progressively more anhydrous. Garnet, Fe–Mn- and Al–Mn-rich sodic pyroxenes are the typical phases of the high-P events.

At the eclogitic peak, apparently under static conditions Mn-jadeite, Mn-omphacite and Mn-aegirine-augite crystallized in the fractures.

The crystallization of Mn hydrate phases (such as richterite, winchite and Mn-phengite in the fractures and in the veins, or piemontite crystallization) occurred late, during the decompressional blueschist event postdating the eclogite climax. For this stage T near 400 °C and P = 8 kbar have been proposed (MARTIN-VERNIZZI, 1982; MOTTANA, 1986).

8.3. GREENSCHIST FACIES EVENT

In the Praborna sequence the greenschist-facies metamorphism developed pervasively only in particular structural domains, along shear zone and where the F3 deformations were penetrative.

During this episode, the fluid circulation contributed to homogenization of the oxidation state of the system. It also mobilized some amounts of manganese and produced Mn-tremolite, Mn-phlogopite, piemontite and rho-

dochrosite crystallization in some late veins and the enrichment in manganese of the epidote, carbonate and garnet of non manganiferous horizons.

Acknowledgements

This study is mainly based on the 3rd cycle thesis (MARTIN-VERNIZZI, 1982) realized in the Laboratoire de Pétrologie of the Pierre et Marie Curie University. Financial support from the Italian M.P.I. is gratefully acknowledged.

We are very grateful to Prof. J. Abrecht, I. Abs-Wurmbach, G.V. Dal Piaz, W.L. Griffin, B. Messiga, A. Mottana and P. Omenetto for the critical reading of the manuscript. We also wish to express our gratitude to I. Abs-Wurmbach, Pascale Vernier, C. Mevel for their suggestions.

References

ABS-WURMBACH, I. (1980): Miscibility and compatibility of braunite $Mn^{2+}Mn^{3+}_6 O_8/SiO_4$ in the system Mn-Si-O at 1 atm in air. Contr. Min. Petr., 71, 393-399.

ABS-WURMBACH, I., PETERS, T.J., LANGER, K. and SCHREYER, W. (1983): Phase relations in the system Mn-Si-O: an experimental and petrological study. Neues Jahrb. Min. Abb., 146, 3, 258-277.

ABS-WURMBACH, I., LANGER, K. and OBERHÄNSLI, R. (1984): Polarized absorbtion spectra of single crystal of the chromium bearing clinopyroxenes cosmochlore and Cr-aegirine augite. Phys. Chem. Min. (in press).

ALT, J.C. and HONNOREZ, J. (1984): Alteration of the upper oceanic crust, DSDP 417: mineralogy and chemistry. Contr. Min. Petr., 87, 149-169.

BEARTH, P. (1964): Atlas der Schweiz 1:25000: Blatt Randa mit Erläuterungen, Schweiz Geolog. Kommission (Bern).

BEARTH, P. (1967): Die Ophiolite der Zone von Zermatt-Saas Fee. «Beitr. Geol. Karte Schweiz», 132, 130 p.

BEARTH, P. (1973): Gesteins- und Mineralparagenesen aus den Ophioliten von Zermatt. Schweiz. mineral. petrogr. Mitt., 53, 299-334.

BEARTH, P. (1976): Zur Gliederung der Bündnerschiefer in der Region von Zermatt-Saas. Eclogae geol. Helv., 69, 149-161.

BEARTH, P. and SCHWANDER, H. (1981): The post-triassic sediments of the ophiolite zone Zermatt-Saas Fee and the associated manganese mineralization. Eclogae geol. Helv., 74/1, 189-205.

BECCALUVA, L., DAL PIAZ, G.V. and MACCIOTTA, G. (1984): Transitional to normal-MORB affinities in ophiolithic metabasites from the Zermatt-Saas, Combin, Antrona units, Western Alps: implications for the paleogeographic evolution of the western Tethyan Basin. Geologie en Mijnbouw, 63/2, 165-177.

BONATTI, E. (1975): Metallogenesis at oceanic spreading centres. Ann. Rev. Earth Plan. Sci., 3, 401-431.

BONATTI, E. (1981): Metal deposit in the oceanic Lithosphere. Emiliani, C. (ed.): The Sea, Wiley, chap. 17, 639-686.

BONATTI, E., ZERBI, M., KAI, R. and RYDELL, H. (1976): Metalliferous deposits from the Apennine ophiolithes: Mesozoic equivalents of modern deposits from oceanic spreading centers. Geol. Soc. Am. Bull., 87, 83-94.

BONDI, M., MOTTANA, A., KURAT, G. and ROSSI, G. (1978): Cristallochimica del violano e della schefferite de St. Marcel (Valle d'Aosta). Rend. SIMP, 34, 15-25.

BROWN, P., ESSENE, J. and PEACOR, D.R. (1978): The mineralogy and petrology of manganese-rich rocks from St. Marcel, Piedmont, Italy. Contr. Min. Petr., 67: 227-232.

BURNHAM, C.W., HOLLAWAY, J.R. and DAVIS, N.F. (1969): Thermodynamic properties of water to 1,000 C and 10,000 bars. Geol. Soc. America Spec. Paper, 132, 96 p.

CABY, R., KIENAST, J.R. and SALIOT, P. (1978): Structure, métamorphism et modèle d'évolution tectonique des Alpes occidentales. Rev. Geogr. Phys. Geol. Dyn., 20, 307-311.

CANN, J.R. (1980): Availability of sulphide ores in the ocean crust. J. Geol. Soc. London, 137, 381-384.

CARPENTER, N.A. (1980): Mechanism of exsolution in sodic pyroxenes. Contr. Min. Petr., 71: 289-300.

CASTELLO, P. (1981): Inventario delle mineralizzazioni a magnetite, ferro-rame e manganese del Complesso Piemontese dei calcescisti con pietre verdi in Valle d'Aosta. Ofioliti, 6/1, 5-46.

CASTELLO, P., DAL PIAZ, G.V., KIENAST, J.R., MARTIN, S., NATALE, P., NERVO, R., POLINO, R. and VENTURELLI, G. (1980): The Piemonte ophiolite nappe in the Aosta Valley and related ore deposits. Field Excursion Guide. VI: Ophiolite Field Conference, G.L.O.M.M., Firenze, 171-192.

CHOPIN, C. (1978): Les paragenèses réduites ou oxidées de concentrations manganésifères des "schistes lustrés" de Haute Maurienne (Alpes Françaises). Bull. Miner., 101, 514-531.

COLOMBA, L. (1910): Sopra un granato ferri-cromifero di Praborna (St. Marcel). Rend R. Acc. Lincei. Roma, 19: 146-150.

CONVERSE, D.R., HOLLAND, H.D. and EDMOND, J.M. (1984): Flow rates in the axial hot spring of the East Pacific Rise (21N): implications for the heat budget and the formation of massive sulphide deposits. Earth Planet. Sci. Lett., 69: 159-175.

CRONAN, D.S. (1980): Metallogenesis at oceanic spreading centres. J. Geol. Soc. London, 137, 369-371.

DAL PIAZ, G.V. (1965): La formazione mesozoica dei calcescisti con pietre fra la Val Sesia e la Valtournanche ed i suoi rapporti con il ricoprimento Monte Rosa e con la zona Sesia-Lanzo. Boll. Soc. Geol. It., 84: 67-104.

DAL PIAZ, G.V. (1974a): Le métamorphisme alpin de haute pression et de basse température dans l'évolution structurale du bassin ophiolitique alpino-apenninique (1re partie: Considérations paléo-

géographiques). Boll. Soc. Geol. It., 93, 437-468.
DAL PIAZ, G.V. (1974b): Le métamorphisme alpin de haute pression et basse température dans l'évolution structurale du bassin ophiolitique alpino-apénninique (2e partie). Schweiz. mineral. petrogr. Mitt., 54, 399-424.
DAL PIAZ, G.V. (1976): Il lembo di ricoprimento del Pillont, falda della Dent Blanche delle Alpi occidentali. Ist. Geol. Mineral. Univ. Padova Mem., 31, 61 p.
DAL PIAZ, G.V. e NERVO, R. (1971): Il lembo di ricoprimento del Glacier-Rafray (Falda Dent Blanche I.S.). Boll. Soc. Geol. It., 90, 401-414.
DAL PIAZ, G.V., DI BATTISTINI, G., KIENAST, J.R. and VENTURELLI, G. (1979): Manganiferous quartzitic schists of the Piemonte ophiolite nappe in the Valsesia-Valtournanche area (Italian Western Alps). Mem. Sci. Geol., 32, 24 p.
DAL PIAZ, G.V. and ERNST, W.G. (1978): Areal geology and petrology of eclogites and associated metabasites of the Piemonte ophiolite nappe, Breuil-St. Jacques area, Italian Western Alps. Tectonophysics, 51, 99-126.
DAL PIAZ, G.V., HUNZIKER, J.C. and MARTINOTTI, G. (1972): La Zona Sesia Lanzo e l'evoluzione tettonico-metamorfica delle Alpi nord occidentali interne. Soc. Geol. It. Mem., 11, 433-466.
DAL PIAZ, G.V., LOMBARDO, B. and GOSSO, G. (1983): Metamorphic evolution of the Mt. Emilius Klippe, Dent Blanche nappe, Western Alps. Am., Jour. Sci., 283-A, 438-458.
DAL PIAZ, G.V., NATALE, E.P., NERVO, R., OMENETTO, P. e POLINO, R. (1978): La mineralizzazione piritoso-cuprifera di Vaifiorcia (Alpi Cozie). Mem. Sc. Geol., Padova, 32, 16 p.
DAL PIAZ, G.V., VENTURELLI, G., SPADEA, P., DI BATTISTINI, G. (1981): Geochemical features of metabasalts and metagabbros from the Piemonte ophiolite nappe, Italian Western Alps. N. Jb. Miner. Abh., 142/3, 248-269.
DELANY, J.M. and HELGESON, H.C. (1978): Calculation of the thermodynamic consequences of dehydratation in subducting oceanic crust to 100 kbar and > 800 C. Am. J. Sci, 278, 638-686.
DEBENEDETTI, A. (1965): Il complesso radiolariti-giacimenti di manganese-giacimenti piritoso-cupriferi-rocce a fuchsite, come rappresentante del Malm nella Formazione dei Calcescisti. Osservazioni nelle Alpi Piemontesi e nella Valle d'Aosta. Bell. Soc. Geol. It., 84, 3-35.
DYMOND, J., CORLISS, J.B., HEATH, G.R., FIELD, G.W., DASCH, E.J. and VEEH, H.H. (1973): Origin of metalliferous sediments from the Pacific Ocean. Geol. Soc. Am. Bull., 84, 3355-3372.
EDMOND, J.M., CORLISS, J.B. and GORDON, L.I. (1979): Ridge crest hydrothermal metamorphism at the Galapagos spreading center andreverse weathering, in Deep Sea Drilling Results in the Atlantic Ocean: Ocean Crust. M. Ewing s.2. Am. Geophys. Union., 383-390.
EDMOND, J.M., VON DAMM, K.L., MCDUFF, R.E. and MEASURES, C.I. (1982): Chemistry of hot springs on the East Pacific Rise and their effluent dispersal. Nature, 297, 187-191.
ERNST, W.G. and DAL PIAZ, G.V. (1978): Mineral parageneses eclogitic rocks and related mafic schists of the Piemonte ophiolite nappe, Breuil-St-Jacques area, Italian Western Alps. Am. Mineral., 63, 621-640.
ESSENE, E.J. and FYFE, W.S. (1967): Omphacite in Californian metamorphic rocks. Contr. Min. Petr., 15, 1-23.
EUGSTER, H.P. and WONES, D.R. (1962): Stability relations of the ferruginous biotite, annite. J. Petrol., 3, 82-125.
GANGULY, J. (1969): Chloritoid stability and related parageneses: theory, experiments and applications. Am. Jour. Sci., 267, 910-944.
GRIFFIN, L.W. and MOTTANA, A. (1982): Crystal chemistry of clinopyroxenes from the St. Marcel manganese deposit, Val d'Aosta, Italy. Am. Miner., 67, 568-586.
HÜBNER, J.S. (1967): Stability relations of minerals in the system Mn-Si-C-O. Dissertation, John Hopkins Univ., Baltimore, Maryland, 279 p.
HÜBNER, J.S. and SATO, M. (1970): The oxygen fugacity-temperature relationships of manganese and nickel oxide buffers. Am. Mineral., 55, 934-952.
HUTTENLOCHER, H.F. (1934): Die Erzlagerstättenzonen der Westalpen. Beitr. Geol. Karte Schweiz. Geotechn. Serie, Nr. 4.
KESKINEN, M. and LIOU, J.J. (1979): Synthesis and stability relations of Mn-Al piemontite, $Ca_2MnAl_2Si_3O_{12}(OH)$. Am. Miner., 64, 317-328.
KIENAST, J.R., TRIBOULET, C. (1972): Le chloritoïde dans les paragenèses à glaucophane, albite ou paragonite. Bull. Soc. Fr. Miner. Cristall., 95, 565-573.
KIENAST, J.R. (1973): Sur l'éxistence de deux séries différentes au sein de l'ensemble «schistes lustrés-ophiolites» du Val d'Aoste, quelques arguments fondés sur l'étude des roches métamorphiques. C.R. Ac. Sc. Paris, 276, 2621-2624.
KIENAST, J.R. (1984): Le métamorphisme de haute pression et de basse température (eclogites et schistes bleus): données nouvelles sur la pétrologie de roches de la croûte océanique subductée et des sédiments associés. Thése d'état. Univ. Paris VI, 484 p.
KIENAST, J.R., MARTIN, S. (1983): I pirosseni egiringiadeitic del livello basale di Praborna, Alpi Occidentali. Ofioliti, 8/2, 245-260.
LATTARD, D. and Schreyer, W. (1983): Synthesis and stability of the garnet calderite in the system Fe-Mn-O. Contr. Min. Petr., 84, 199-214.
LEAKE, B.E. (1978): Nomenclature of amphiboles. Bull. Soc. Fr. Mineral. Cristallograf., 101, 453-467.
LIOU, J.G. (1973): Synthesis and stability relations of epidote, $Ca_2Al_2FeSi_3O_{12}(OH)$. J. Petrol., 14, 381-413.
MARTIN-VERNIZZI, S. (1982): La mine de Praborna (Val d'Aoste, Italie): une série manganésifère métamorphisée dans le faciés éclogite. Thèse 3e cycle. Univ. Paris VI., 430 p.
MARTIN, S., KIENAST, J.R. (1983): Les augite-aegyrines chromifères de Praborna, Val d'Aoste, Italie. Ofioliti, 8, abstract.
MARTIN, S. e POLINO, R.: Le metaradiolariti a ferro di Cesana (Valle di Susa, Alpi Occidentali). Mem. Soc. It., atti 72 Congresso, Torino, 1984, in stampa.
MOORBY, S.A., CRONAN, D.S. and GLASBY, G.P., (1983). Geochemistry of hydrothermal Mn-oxide

deposits from SW Pacific island arc. Geochem. Cosmochic. Acta., 48, 433-441.

MOTTANA, A. (1986): Blueschist-facies metamorphism of manganiferous cherts: A review of the alpine occurrences. Geol. Soc. Am., Mem. 164, 267-299.

MOTTANA, A., ROSSI, G., KRACHER, A. and KURAT, G. (1979): Violan revisited: Mn-bearing omphacite and diopside. Tscherm. Min. Petr. Mitt., 26, 187-201.

MOTTANA, A. and GRIFFIN, W.L. (1983): The crystal-chemistry of piemontite from the type-locality (St. Marcel, Val d'Aosta, Italy). International Mineralogical Association for its 13th Meeting at Varna, Bulgaria.

MOTTANA, A. and GRIFFIN, W.L. (1985): The crystal chemistry of two high-pressure potassium richterites. Terra Cognita, 5, 2/3, 327.

MOTTL, M.J. (1983): Metabasalts, axial hot springs, and the structure of hydrothermal systems at mid-ocean ridges. Geol. Soc. Am. Bull. 94, 161-180.

MUAN, A. (1959): Phase equilibria in the system manganese oxide-SiO_2 in air. Amer. J. Sci., 57, 1280-1282.

PAPIKE, J.J., CAMERON, K.L., BALDWIN, K. (1974): Amphiboles and clinopyroxenes: characterization of other than quadrilateral components and estimates of ferric iron from microprobe data. Geol. Soc. Am. Abstr. Progr., 6, 1053-1054.

PENFIELD, S.L. (1893): Some minerals from the manganese mines of the St. Marcel, Italy, Amer. Jour. Sci., 3, 46, 288-295.

PERSEIL, E.A. (1985): Quelques caractéristiques des faciès de manganèse dans le gisement de St. Marcel-Praborna-V. Aosta, Italie. Miner. Deposita, 20/4, 271-276.

PERSEIL, E.A, KIENAST, J.R. (1982): Sur quelques aspects de l'évolution des oxides dans le gisement de St. Marcel, Val d'Aoste, Italie. Terra Cognita, 2/3, 344 p.

RICHARDSON, S.M. (1975): A pink muscovite with reverse pleochroism from Archer's Post, Kenya. Am. Mineral., 60, 73-78.

RISE PROJECT GROUP (1980): East Pacific Rise: Hot Springs and Geophysical Experiments. Science, 207, n. 4438.

ROBERTSON, A.H.F. and HUDSON, J.D. (1974): Pelagic sediments in the Cretaceous and Tertiary history of the Troodos Massif, Cyprus. Spec. Publ. Int. Assoc. Sedimentol., 1, 403-436.

RONA, P.A., HARBISON, R.N., BASSINGER, B.G., SCOTT, R.B. and NALWALK, A.J. (1976): Tectonic fabric and hydrothermal activity of Mid-Atlantic-Ridge crest (lat. 26 N). Bull. Geol. Soc. Am., 87, 661-674.

RONA, P.A. (1980): TAG hydrothermal Field: Mid-Atlantic Ridge crest at latitude 26 N. J. Geol. Soc. London, 137, 385-402.

RONDOLINO, R. (1936): Sopra alcuni anfiboli manganesiferi di Praborna (St. Marcel, Valle d'Aosta). Period. Mineral., 7, 109-121.

SIVAPRAKASASH, C. (1980): Mineralogy of Manganese Deposits of Koduru and Garbham, Andhra Pradesh, India. Econ. Geol., 75: 1083-1104.

TARTAROTTI, P., MARTIN, S. and POLINO, R. (1987): Field data in the St. Marcel valley (Aosta valley), Ofioliti, 11 (3), 343-346.

TRÜMPY, R. (1980): Geology of Switzerland: A guidebook, Wepf, Basel, Switzerland.

Manuscript received March 12, 1987; revised manuscript accepted December 18, 1987.